NTNU

Norwegian University of
Science and Technology

Development of Bio-Oil Emulsion to Allow Realistic Testing of Oil Spill Control Equipment

Turan Eyyubbayli

Petroleum Engineering
Submission date: October 2015
Supervisor: Harald Arne Asheim, IPT

Norwegian University of Science and Technology
Department of Petroleum Engineering and Applied Geophysics

Abstract

Accidental release of oil to the sea poses may have dire ecological consequences and serious economic ramifications, as recent events have shown. Spill control equipment as: booms, skimmers and oil trawls may protect sensitive areas and remove floating oil. This is subject to continuous technological development and innovation.

To support such development there is a pressing need to test new equipment under realistic conditions; in other words by release of oil to find out if can be successfully removed. Intentional release of crude oil to the sea will usually be taboo. If the crude is replaced by edible oil, reasons for restrictions are far less.

Subjected to wavy sea, most crudes will develop stable non-Newtonian emulsions of considerable stiffness. Using soybean oil and an emulsifier, stable bio-emulsion with similar density and rheological properties were developed. Microscopic image analyzes showed that the emulsions consisted of water droplets in the typical range 5-20 microns, surrounded by a thin oil film. The droplet approximately followed the lognormal distribution. The water content could be up to 70%, yet the emulsions were oil-continuous and very stable.

Obviously, the potential benefits of using such emulsions for equipment development and verification are high and the environmental impact is probably small and possibly beneficial. So permission for limited tests at sea in August has been given by Norwegian authorities and was performed in north of the Vesterålen islands in September 2014.

Preface

The experimental procedure together with the results and conclusion of it is published and presented in SPE Latin American and Caribbean Health, Safety, Environment and Sustainability Conference held in Bogota, Colombia, 7-8 July 2015. (SPE-174131-MS)

Acknowledgement

This thesis has been carried out at the Department of Petroleum Engineering and Applied Geophysics, Norwegian University of Science and Technology (NTNU). The thesis is the final product of TPG4920 – Master's Thesis in Petroleum Engineering.

First of all I would like to express a sincere gratitude to my supervisor Prof. Harald Arne Asheim for giving me the opportunity to conduct this study, for his guidance, help with experiments and writing process. Special thanks to Knut Gaaseidnes from Reninor AS and Hugo Svendsen from NorLense AS for their coaching and guidance. I would also like to thank Randi Utgård from Biotechnology Department for helping me how to work with the microscope Zeiss Axio Imager.

I also would like to thank my friends, Aysel Heydarova, Farad Kamyabi and Murad Babayev, who were so supportive and generous. They always kept my moral high and motivated me to complete my thesis work.

It is a pleasure to acknowledge with gratitude the financial support of Norwegian Government for two years of International Master's Program.

Turan Eyyubbayli

Table of Contents

List of Figures

Nomenclature

τ	Shear Stress
γ	Shear Rate
τ_0	Yield Stress
μ	Viscosity
τ_{gel}	Gel Stress
n	Flow Behavior Index
K	Consistency Index
A	Area
V	Volume
v	Velocity
h	Distance

1. Introduction

Nowadays, developing science and technology is showing that any oil spill to the sea surface is more hazardous than expected. Therefore, there exists a lot of ongoing research to mitigate with this issue. Recent studies showed that oil is weathered and emulsified on the sea surface. In order to test oil spill response equipment environmentally friendly, sample must be made which would be used as a substitute to the crude-oil emulsion. In most cases this will be the preferred solution for protecting sensitive areas. This is a traditional technology, but subject to continuous development and streamlining to extend its applications to larger spills and more weather exposed areas.

The basic mechanism of removing floating oil spill is akin to the skimming of floating fat from a soup. But as there are obvious differences between a soup kettle and the open sea, larger test facilities are essential. Such mechanisms have been built at several locations and provide a fundament for technology development.

Largest test tanks, like the Ohmsett facility measuring 203x20x3.4 meter, enable equipment verification under controlled conditions. However, even facilities of such dimensions cannot mimic the conditions and loads of the open sea.

Oil-on-Water exercises are conducted yearly in the Frigg field area offshore Norway using actual crude-oil emulsions. Such full testing of equipment and operations procedures may identify of weaknesses better than tank testing. However, since such tests are expensive and rare, admission is selective and limited. So it may be argued that more available testing possibility will stimulate the development of oil spill control technology.

The simplest and most realistic approach to testing is to release of oil to the sea, to see if can be successfully removed. Crude oils are generally harmful to life, and intentional release will usually be taboo. However, if the crude is replaced by edible bio-oils, the reasons for restrictions will be less.

To find out if crudes can be substituted with bio-oils, it is necessary to find out if bio-oil emulsions can be made with rheological properties comparable to the emulsions formed by crude oil and sea water. This is investigated here.

2. Theory

2.1. Fluid Rheology

Rheology defined as the study of deformation and flow matter. For the liquids rheological properties are flow and deformation responses of rheological properties are based on flow and deformation responses of liquids when subjected to normal and tangential stresses.

"The resistance which arises from the lack of slipperiness of the parts of the liquid, other things being an equal is proportional to the velocity with which the parts of the liquid are separated from one another. This lack of slipperiness is what we now call 'viscosity'. It is synonymous with "internal friction" and is a measure of "resistance to flow"." (Barnes et al., 1989)

To understand the concept of Viscosity, we can assume two horizontal plates placed with distance of h between each other. To assume that first plate will move with the velocity u_1 by applying external force F (which is not so big). At the same time the liquid layer touching to the first plate will have the speed u_1 and the liquids below will join that movement due to the friction force initiated by chaotic thermal motion of molecules and the existing cohesion force between them (see figure 1).

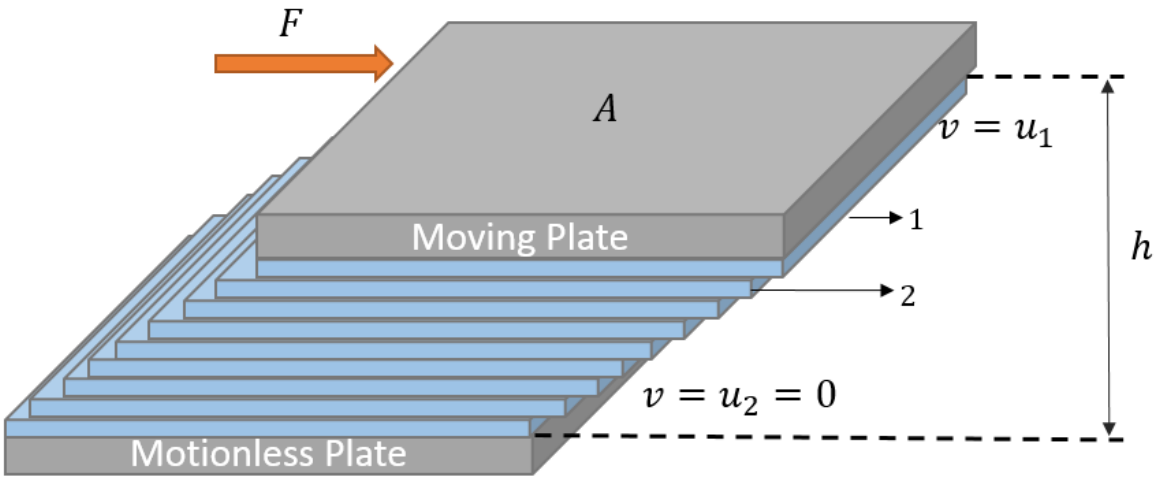

Figure 1: The graphic illustrates flow of fluid between two plates of area A. The bottom plate is motionless. When the top plate is moved to the right, it drags the fluid along with it.

However, the below liquid layers will tend to stop upper moving liquids for this reason the speed in upper layers will be more than the below layers. Each layer of fluid will move faster than the one below it, and friction between the layers will give rise to a force which resists to their relative motion. The speed of fluid will become zero on the Second motionless plate.

For the liquids at radial laminar flow, speed distribution of liquid particles depending on cross section radius is shown in figure 2. In this case speed of liquid layers touching to the pipe wall will be zero and in center of pipe liquid will have maximum speed.

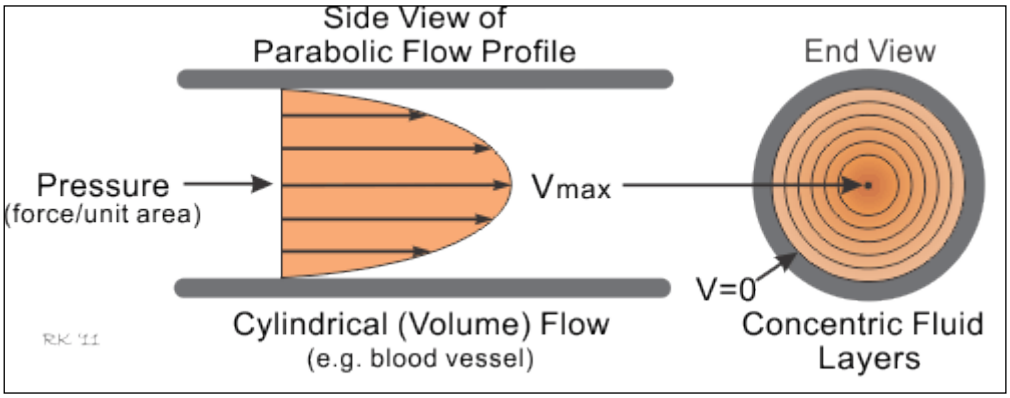

Figure 2: Velocity distribution in laminar flow (http://www.cvphysiology.com/Hemodynamics/H006.htm).

1 and 2 are very close liquid layers and their velocities are u_1 and u_2. Distance between them which are dx and $\frac{du}{dx}$ is velocity gradient.

According to the Newton, internal friction force F in layered moving liquid is proportional with area A of force applied and speed gradient

$$F = \pm\mu A \frac{du}{dx} \qquad (1)$$

Or

$$F = \pm\mu A \frac{du}{dr} \qquad (2)$$

Where, $\frac{du}{dx} = \dot{\gamma}\ and\ \frac{du}{dr} = \gamma$

$$F = \pm\mu A\gamma \qquad (3)$$

Here, μ is dynamic viscosity γ is the shear rate and A is the cross sectional area and $\pm$ are dependent on velocity gradient.

Viscosity derived from formula (4) as follows:

$$\mu = \frac{F}{\pm A\gamma} \qquad (4)$$

Therefore, when $A = 1$ and $\gamma = 1$ then $F = \mu$, for this reason viscosity can be measured by friction force. Ratio of friction force to the unit of area could be equal to shear stress (τ).

Shear stress expressed as:

$$\tau = \frac{F}{A} = \pm\mu\gamma \qquad (5)$$

So, dependence between τ and γ will be linear. From the figure 3, $ctg(\beta) = \mu$.

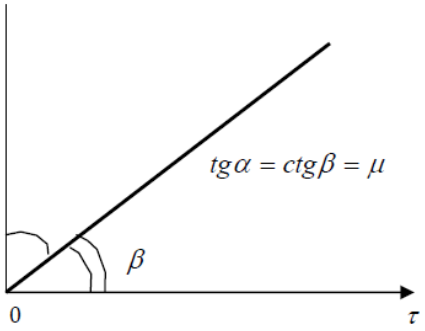

Figure 3: Share stress vs shear rate.

The unit of dynamic viscosity is P$a * s$, the old unit Poise is still used widely named after J. L. M. Poiseuille, a French physician who performed experiments in 1840 on water flow in pipes.

Beside dynamic viscosity kinematic viscosity is used as well.

$$v = \frac{\mu}{\rho}, \left(\frac{m^2}{s}\right) \qquad (6)$$

In SI system, kinematic viscosity is reported using Stokes (St) and $10^{-4}\frac{m^2}{s}$=1 St. Stokes is a large unit, and it is usually divided by 100 to give the unit called Centistokes (cSt) (Mirzadzhanzade, 1990).

Classification of Fluids

Fluids are normally classified into four categories, according to the relationship between the shear stress and shear rate:

1- Newtonian fluids
2- Time-independent non-Newtonian fluids
3- Time-dependent non-Newtonian fluids
4- Viscoelastic fluids

Newtonian fluids

When the viscosity of a liquid remains constant and is independent of the applied shear stress, such a liquid is termed a Newtonian liquid (see figure 4).

Time-independent non-Newtonian fluids

Non-Newtonian fluids in general, include thickened water and gelled fluids. The term 'non-Newtonian' implies that the viscosity is not only dependent to the pressure and temperature but also on the rate of shear that is applied to the fluid.

Non-Newtonian fluids related to petroleum engineering especially in the injection of fluids in different oil recovery operations. In addition these kinds of liquids sometimes circulated in drilling process.

From relationship of viscosity with shear rate time dependent non-Newtonian fluids can be classified as follows (Figure 4).

Pseudo-plastic fluids

The apparent viscosity (AV) of the fluid is inversely proportional with shear rate which means shear rate increases with decreasing AV. This behavior of fluids also calls "shear thinning" behavior, and for these fluids yield stress is not required to initiate shearing. Grease, molasses, paint and starch are Pseudo plastic fluids. Most of the oil in water emulsion behaves like pseudo-plastic and they follow Power Law. (Pal and Rhodes, 1989). According to Pal & Rhodes, at lower concentrations of dispersed phase (<20%), the emulsions behaved like Newtonian fluids where at higher concentrations, the emulsions behaved like pseudo-

plastic fluids. The flow curves of shear stress versus shear rate were found to follow a linear relationship on a log-log plot (Pal and Rhodes, 1985).

Dilatant fluids

The AV of the fluid is proportional with shear rate which means shear rate increases with increasing AV. This behavior of fluids also calls "shear thickening" behavior, and for these fluids yield stress is not required to initiate shearing. Peanut butter can be a good example for dilatant fluids.

Visco-plastic fluids

Visco-plastic fluids are normally exhibit a yield stress. Shear stress plays a great role for visco-plastic fluids. Below a certain critical shear stress no deformation of the fluids happens and fluid behaves like a rigid solid. Oppositely, above the critical stress the material flows like a fluid. One special case of dilatant fluids are Bingham plastic fluids. An example for Bingham fluid can be toothpaste which needs applied force, squeezing, to initiate flow.

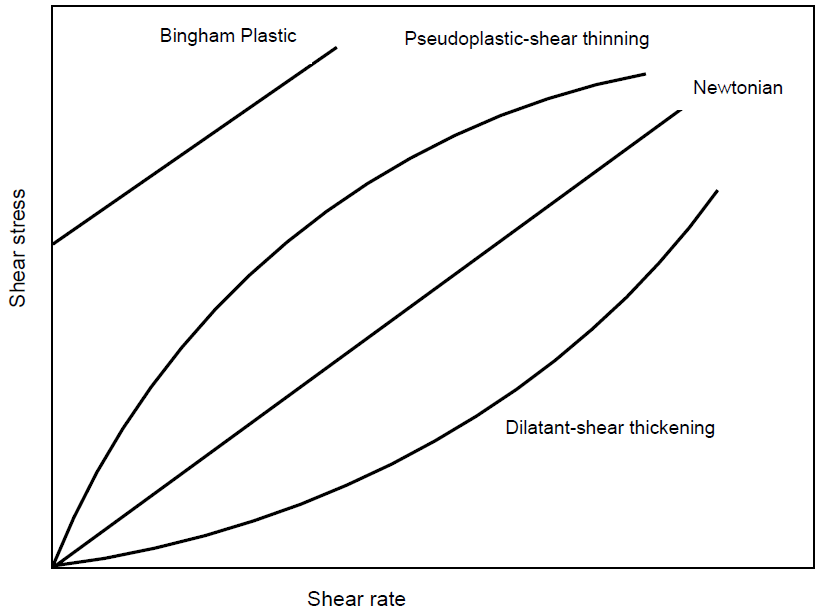

Figure 4: Rheological behavior of various types of non-Newtonian fluids.

Time-dependent non-Newtonian fluids

Time dependent non-Newtonian fluids are influenced by the time factor (recent past). These fluids show a "memory" that weakens with time. The apparent viscosity (AV) of these non-

Newtonian fluids are dependent upon on different properties such as, shear rate, history of shearing process, the shape of the place that it flows. From relationship of apparent viscosity with time these fluids can be classified as follows:

Thixotropic fluids

A thixotropic fluid displays a reduction in AV over time at constant shear rate. When shear rate is removed, the AV gradually rises and returns to its initial value. Cement and drilling fluids have a thixotropic behavior. It can include most of w/o emulsions. In figure 5, behavior of thixotropic fluid is illustrated.

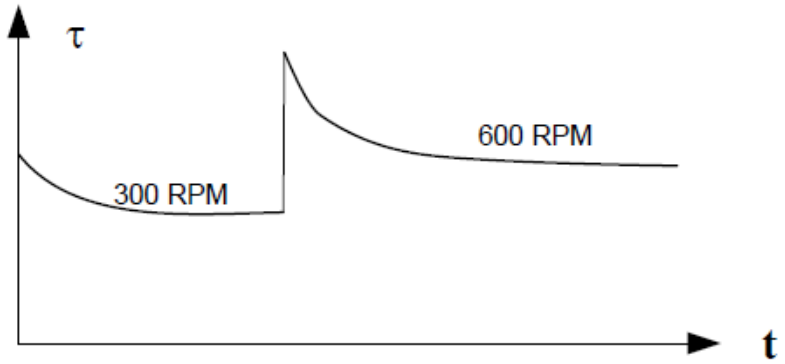

Figure 5: Behavior of thixotropic fluids after stillstad (left) and at constant shear rates (Skalle, 2012).

Rheopectic fluids

A rheopectic fluids behave in opposite way of thixotropic fluids which means rheopectic fluids displays an increasing shear stress at increasing shear rate and at increasing time at constant shear rate. When shear stress is removed, the AV gradually reduces and returns to its initial value. In nature rheopectics fluids are rare and an example can specific gypsum paste or printer ink. Comparasion of viscosity dependence from time is shown Figure 6.

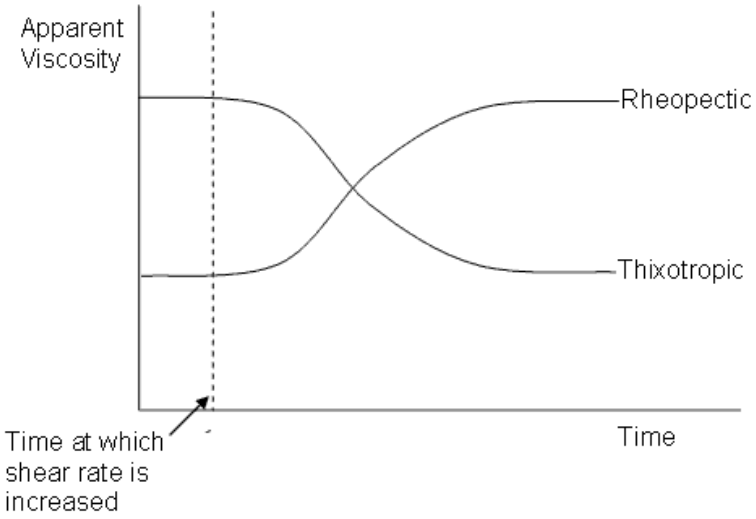

Figure 6: Rheopectic fluids as the opposite of thixotropic fluids
http://www.tececo.com/files/newsletters/Newsletter34.htm

Mathematical Fluid Models

Mathematical Fluid Models are mathematical relationships between shear rate and shear stress. While the relationship is constant for the Newtonian fluids, it becomes more complicated for the Non-Newtonian fluids. Several models have been introduced, which is still not accurate enough to describe Non-Newtonian fluids. Two mainly used Non-Newtonian models are Bingham Plastic and Power Law Model. Additional models described are the Casson Model, the Robertson-Stiff Model, and the Herschel-Bulkley Model (see figure 7).

Bingham Model

Bingham model assumes that deformation takes place after the shear stress exceeds the yield point. After the yield point Bingham model suggest that the rate of shear and shear stress are continue linearly. But for the pseudo plastic fluid the shear stress increases with shear rate at less than linear rate, in that respect Bingham model is not applicable for all the applications of non-Newtonian fluids.

Bingham Model could be used for fluids exhibit plastic behavior. Yield stress is requires to initiate the flow.

$$\tau = \tau_0 + (\mu_\infty)(\gamma) \qquad (9)$$

Where, τ =shear stress , τ_0 =yield point, μ_∞=Plastic viscosity, γ = shear rate. (Skalle, 2012)

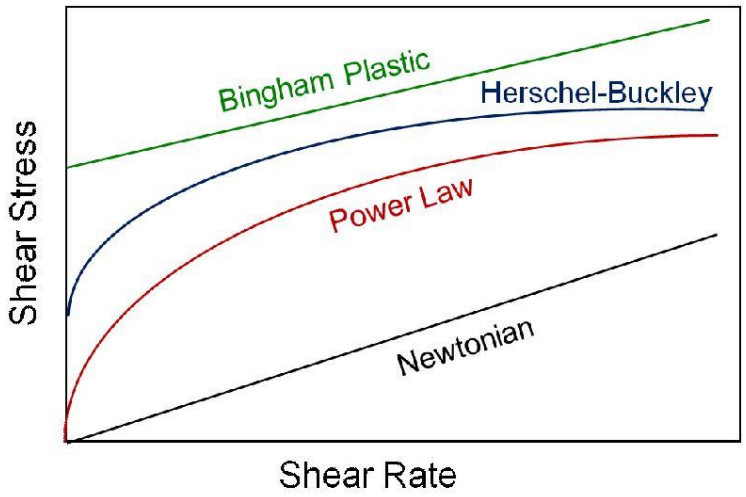

Figure 7: Rheological models for fluids. (http://www.intechopen.com/books/effective-and-sustainable-hydraulic-fracturing/fracturing-fluids)

Power Law

The power law which is based on the assumption that the rate of shear is proportional to the nth power of the shearing stress is often used as a generalized non-Newtonian fluid model (Olarewaju). It is given by the following relationship between the flow behavior index n, and the consistency index K as:

$$\tau = K\gamma^n \qquad (10)$$

The flow behavior index varies between 0 to 1 for non-Newtonian fluids and when n=1 the fluid considered Newtonian fluid. Power law non-Newtonian flow model commonly used in polymer flooding. In non-Newtonian fluids when the shear rate is low, the particle interference is high and the fluid tends to flow more like a solid mass. In such a case the velocity profile is flattened. This flattening of the velocity profile increases the sweep efficiency of a fluid in displacing another fluid (Ikoku and Ramey).

The power-law constants *(K* and *n)* could be determined by linear regression, and were used to calculate the viscosities of emulsions at various shear rates. (Pal and Rhodes, 1989)

Herschel-Bulkley

Herschel-Bulkley (Yield-Power Law) – Most of emulsions display characteristics of both Pseudo-plastic and thixotropic fluids. Herschel-Bulkley could be expressed below equation:

$$\tau = \tau_y + K\gamma^n \qquad (11)$$

Where τ_y is the YPL yield stress (a better approximation to the true yield stress than the yield point inthe Bingham model), and K and n are the Herschel-Bulkley consistency index and exponent, respectively. The Herschel-Bulkley model may be thought of as a combination of the Bingham Plastic and Power Law pseudo-plastic models, but the Bingham plastic component may also be seen as a manifestation of thixotropic behavior.

When τ_y is zero, the Herschel-Bulkley model reduces to the Power-Law Model for pseudo-plastic flow, and when n is one, it reduces to the Bingham model (Skalle, 2012).

Gel Strength and Yield Point

"The yield value (expressed in lbf/100 ft2 or Pa) is a measurement of the attractive forces that exist between the particles in a fluid while under flowing conditions. The *gel strength* is a measure of the attractive forces between the particles in a fluid under static conditions". In other word, difference between yield point and gel strength in term of hydraulics is that gel strength will not exist once the fluid is moving and the gel has been broken, while the effects of YP will not disappear when the fluid is moving. It indicates thixotropic properties of fluid and represents the minimum shear-stress value-τ_{gel}, necessary to induce flow (Nelson and Guillot, 2006).

Gel strength in a fluid depends on chemical treatments, solid concentration, time, and temperature. "Many workers have studied the measurement of yield stress, but there is a general disagreement between different methods used. In fact, it is a common occurrence at British Society of Rheology meetings, as well as international conferences, that there is heated discussion as to whether yield stress exists at all. Some asserted that yield stress exists as a well-defined quantity Whether the yield stress actually exists or not, it is too important an industrial and engineering parameter to disregard, but it must be realised that absolute values of yield stress cannot be obtained as its magnitude may vary according to the experimental or practical conditions (Cheng, 1986).

2.2. Emulsions

IUPAC definition: “An emulsion is a dispersion of droplets of one liquid in another one with which it is incompletely miscible. Emulsions of droplets of an organic liquid (an “oil”) in an aqueous solution are indicated by the symbol O/W and emulsions of aqueous droplets in an organic liquid as W/O. In emulsions the droplets often exceed the usual limits for colloids in size” (Shinoda and Friberg, 1986).

Emulsions are one of the most intriguing subjects for rheological investigations due to their combination of various properties, such as non-Newtonian behaviour, elasticity, time-dependent effects and so on. The term “emulsions” formally describes a great number of blends of immiscible liquids, including polymeric substances. However, as a general rule, one means mixtures of low molecular weight components (such as water and oil). Emulsions of different types are widely spread in different branches of technology including food processing, pharmaceuticals, enhanced oil recovery and are frequently encountered in biological systems. Two main classes of emulsions are distinguished—water-in-oil (w/o) and oil-in water (o/w) emulsions, although intermediate cases can be also found. This paper is devoted to w/o type emulsions.

Such emulsions consist of droplets of the water-containing phase dispersed in an organic liquid, which comprises of the continuous external phase. This system can only be stable if the water droplets are covered with surfactant (or emulsifier). So, w/o emulsions are complex multi-component and multi-phase systems (Masalova et al., 2003).

The rheological properties of an emulsion are strongly dependent on the morphology (Lacroix et al., 1997).

Emulsions are a class of two immiscible liquids, which one disperses in the other. The disperse phase containing liquid droplets are dispersed in the continuous phase. Oil-in-water (O/W), water-in-oil (W/O), and oil-in-oil (O/O) are the various classes of emulsions (see figure 8) Polar oil dispersed in a nonpolar oil and vice versa may be a good example for O/O class. Emulsifier is needed as a third component to disperse two immiscible liquids. The essential step is choosing the emulsifier when it comes to the formation of the emulsion and its long-run stability.

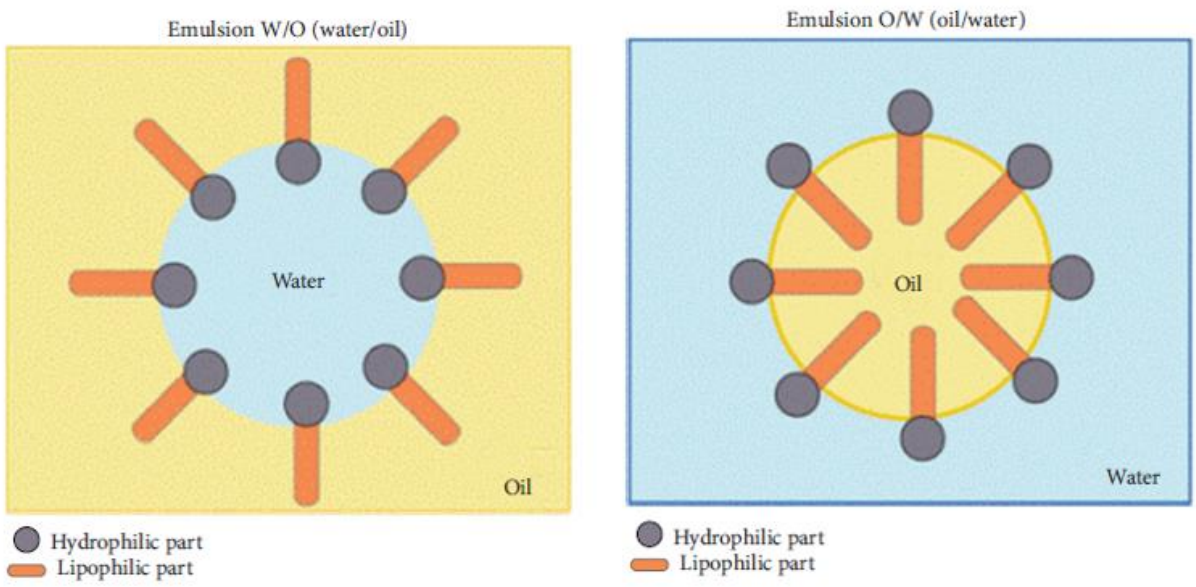

Figure 8: Types of emulsions (Josefa et al., 2013)

Nature of the emulsifier and the structure of the emulsion system are needed to classify the emulsions. This is illustrated in Table 1 (Tadros, 2013). In case of forming emulsions from crude oil, asphaltenes and resins could be surface active agents. Therefore, emulsions form often in the mixture of crude oil with water (Wang et al., 2013).

Table 1: Classification of emulsifier

Nature of emulsifier	*Structure of the system*
Simple molecules and ions	***Nature of internal and external phase: O/W, W/O***
Nonionic surfactants	***----***
Surfactant mixtures	***Micellar emulsions (microemulsions)***
Ionic surfactants	***Macroemulsions***
Nonionic polymers	***Bilayer droplets***
Polyelectrolytes	***Double and multiple emulsions***
Mixed polymers and surfactants	***Mixes emulsion***
Liquid crystalline phases	***----***
Solid particles	***----***

Nature of the Emulsifier

Nonionic surfactants regarded as the most useful emulsifier can be applied to emulsify O/W or W/O. Moreover, they can make the emulsion stable against coalescence and flocculation. Besides nonionic surfactants ionic ones can also be employed as emulsifiers. By mixing ionic and nonionic, or several nonionic surfactants more effectual surfactant mixtures can be attained for emulsification and stabilization of the emulsion. Nonionic polymers are more efficient to get emulsion stability. All the same, these polymers may experience the difficulty

of emulsification if there is not applied high energy for the process. Polyelectrolytes can be utilized as emulsifiers. The ideal state in succeeding simplicity of emulsification and emulsion stability is composition of surfactants and polymers. To maintain emulsion stability lamellar liquid crystalline phases derived from surfactant mixtures are very efficacious. At the O/W interface solid particles gather which can be utilized for stabilizing the emulsions are referred to as Pickering emulsions.

Structure of the System

1) *O/W and W/O macroemulsions*: These usually have a size range of 0.1–5 μm with an average of 1–2 μm.
2) *Nanoemulsions:* these usually have a size range of 20–100 nm. Similar to macroemulsions, they are only kinetically stable.
3) *Micellar emulsions or microemulsions:* these usually have the size range of 5–50 nm. They are thermodynamically stable.
4) *Double and multiple emulsions:* these are emulsions-of-emulsions, W/O/W, and O/W/O systems.
5) *Mixed emulsions:* these are systems consisting of two different disperse droplets that do not mix in a continuous medium (Tadros, 2013).

Stability loss in emulsions

Emulsion stability usually needs the existence of surface-active molecules or small solid particles which precludes the coalescence of droplets. To attain stable emulsions is the major interest in several fields, such as food industry, paint production. On the contrary, for oil recovery destabilization and separation of oil is required. Four different stability loss is observed in emulsion (Petsev, 2004).

Creaming and Sedimentation

External forces such as gravitation and centrifugal forces can bring about cremaing and sedimentation (Figure 9). When external forces surpass the thermal movement of the droplets, a concentration gradient in the system increases, and the larger droplets with the lower density than medium move faster to the top, and those with the larger density than medium change their position to the bottom of the container (Tadros, 2013). In O/W emulsion the accumulation of the oil droplets at the top forms a cream layer (Petsev, 2004).

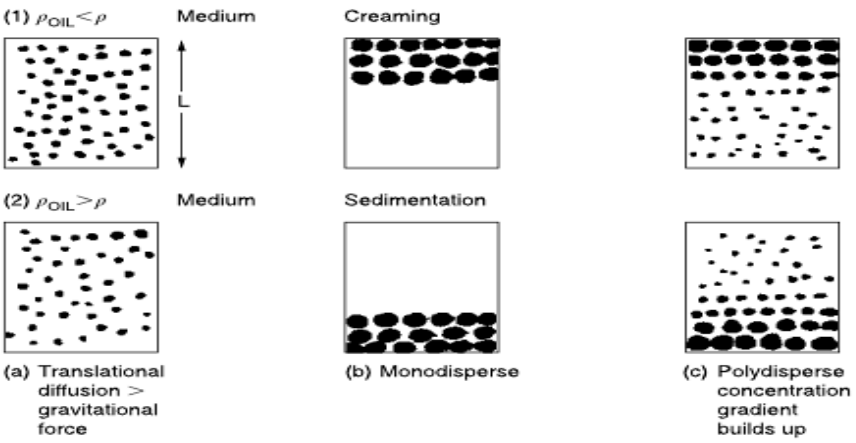

Figure 9: Representation of creaming and sedimentation (Tadros, 2013).

Flocculation

Flocculation is the process of aggregation or accumulation of the droplets into bigger units without modifying their primary size. Flocculation occurs as a result of van der Waals attraction. When there is not adequate repulsion to make droplets stay apart from each other it may cause flocculation (Tadros, 2013). Considering the magnitude of the attractive energy included, it may result in "strong" or "weak" flocculation. Compact or having an enlarged gel-like structured aggregates could present. A thin liquid film makes the individual droplets stay separated from each other. Individual droplets Flocculation can be characterized as weak and reversible or strong irreversible. By forming larger flocks flocculation may induce creaming. Additionally, flocculation is regarded as a precondition for coalescence (Petsev, 2004).

Ostwald Ripening (Disproportionation)

As a result of the limited solubility of the liquid phase disproportionation may occur. Immiscible liquids generally have mutual solubilities that are not insignificant. Due to curvature effects with polydisperse emulsions larger droplets will have smaller solubility compared to smaller ones. Later the smaller droplets deposit on the larger ones by disappearing and diffusing to the bulk (Tadros, 2013).

Coalescence

Coalescence occurs when liquid layer between droplets becomes thinner and ends up with merging two or more droplets into single larger one. When the emulsion becomes utterly separated into two discrete liquid phases it can be considered as a restrictive case for coalescence. Film or surface fluctuations which cause nearly tight approach of the droplets in accordance with strong van der Waals forces precluding their separation are the driving forces for coalescence (Tadros, 2005). In coalescence continuous phase does not separate the droplets and they grow into a single entity. The attractive forces, or hydrodynamic instabilities may be a reason for the detachment of the liquid film between droplets which before separated them in flocculation (Petsev, 2004).

Emulsifiers

An emulsifier is a substance that stabilizes an emulsion by increasing its kinetic stability. One class of emulsifiers is known as “surface active agents”, or surfactants.

The emulsifying agent creates a film over one phase that forms globules, which repel each other. This repulsive force causes them to remain suspended in the dispersion medium.

Methods of Emulsification

For emulsion preparation various procedures can be employed, they can be simple pipe flow (low agitation energy L); static mixers and general stirrers (low to medium energy, L–M); high-speed mixers such as the Ultraturrex (medium energy, M); colloid mills and high-pressure homogenizers (high energy, H); and ultrasound generators (M–H). The preparation method can be continuous (C) or batch-wise (B):

1.Continuous (C): pipe flow and static mixers; high-pressure homogenizers;

2.Continuous (C) or batch-wise (B): stirrers and Ultraturrax; ultrasound (Tadros, 2013).

Synthetic emulsifiers

PGPR

Naturally occurring fats or oils exposed to various chemical processes are considered as semi-synthetic emulsifiers (Coultate, 2009).

PGPR is a food additive, has the code of E-476, used as emulsifier in tin-greasing emulsions and for the synthesis of low-fat spreads. Whereas, PGPR is mainly used in the chocolate industry, where its emulsifier and viscosity modifier features are important. Because of its stable emulsification ability even at the very high water content, the PGPR is also known as a significant water-in-oil emulsifier. Additionally, PGPR is used as a water-in-oil emulsifier to synthesize low-fat spreads. (Josefa et al., 2013).

The lecithin is frequently replaced by polyglyceryl polyricinoleate (PGPR) in chocolate. PGPR is synthesized from glycerol and ricinoelic acid (from castor bean oil). However the end product consists of individual molecules varying in number of glycerol residues and ricinoleic acid residues. Figure 10 illustrates the chemical structure of polyglyceryl polyricinoleate. (Coultate, 2009). In figure 11, the effect of concentration of PGPR is shown.

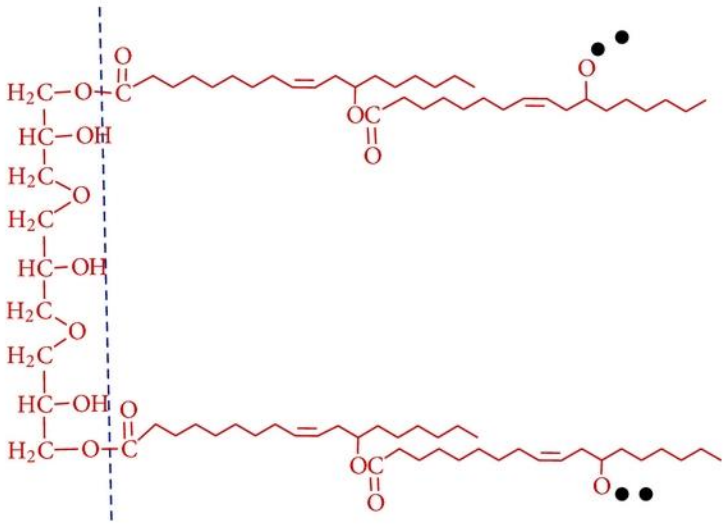

Figure 10: Chemical structure of PGPR. Black dots denote polyricinoleic acid chains (Coultate, 2009).

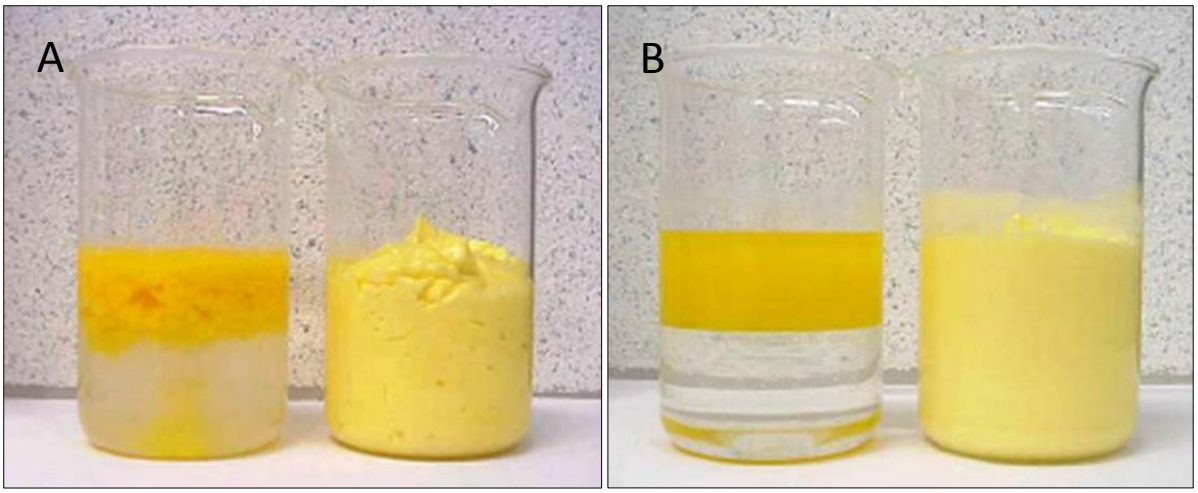

Figure 11: Example of a low-fat spread based on 20% fat and containing milk powder, gelatin, and sodium alginate. (A) 1% distilled monoglyceride (up) and 0.6% distilled monoglyceride + 0.4% PGPR (right). (B) 0.6% distilled monoglyceride (Down) and 0.4% distilled (Josefa et al., 2013).

Factors affecting Crude Oil Emulsion

Viscosity of the emulsions increased by increasing the oil content of the emulsion, surfactant concentration, speed and time of mixing, salt concentration, and pH of the aqueous phase, while temperature of homogenization process substantially reduced the viscosity of the prepared emulsion

The stability of crude oil-in-water emulsions decreased by increasing the oil content while increasing the surfactant concentration, time and speed of mixing, pH of the aqueous phase and temperature enhanced the emulsion stability. The stability of crude oil emulsions was also increased by increasing the salt cconcentration (Ashrafizadeh and Kamran, 2010).

Effect of oil concentration

Increasing oil concentration coincides with an increase viscosity of water in oil emulsion. This could be explained as an increase number of oil droplets which leads contact surface become larger between droplets shown in figure 12 (Azodi and Solaimany Nazar, 2013).

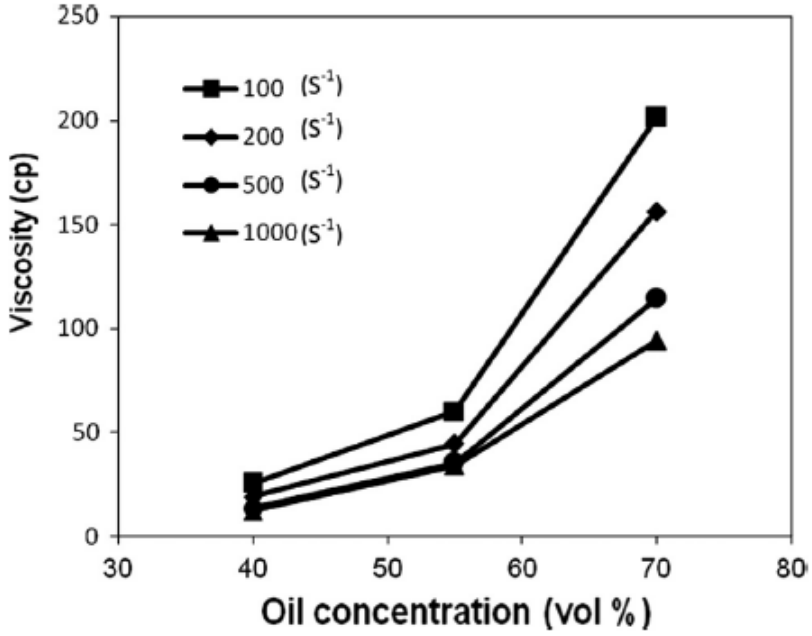

Figure 12: Effect of oil concentration on viscosity of emulsion of oil type 1 at 100, 200, 500 and 1000 (s^{-1}) shear rates (Azodi and Solaimany Nazar, 2013).

Effect of salinity

In 1999, Ahmad *et. al* have observed that the viscosity of the emulsion prepared from fresh water is always less than that prepared from formation water (Figure 14). The reason why the viscosity increases while water salinity rises may be explained by the fact that the interfacial tension is low in saline water which decreases average particle size of dispersed oil. As a result, dynamic shear viscosity increase is detected (Ahmed et al., 1999). Ashrafizadeh and Kamran (2010) have also observed that increase in salt concentration leads to increased viscosity and stability of crude oil emulsion (Figure 13).

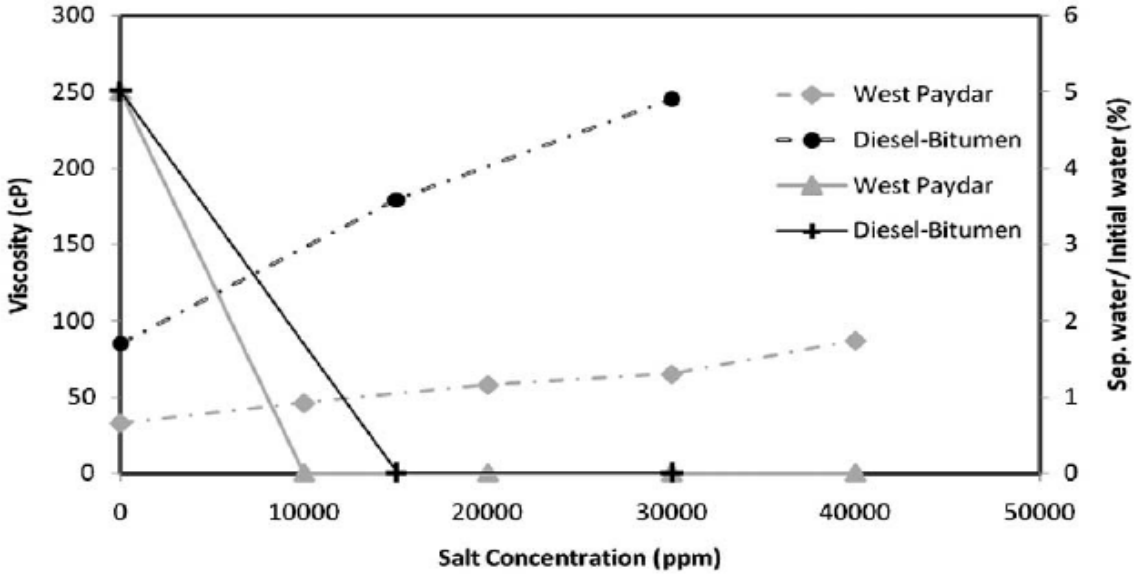

Figure 13: Effect of salt concentration on the viscosity and stability of Iranian oil sample emulsions (dashed lines present viscosity) (Ashrafizadeh and Kamran, 2010).

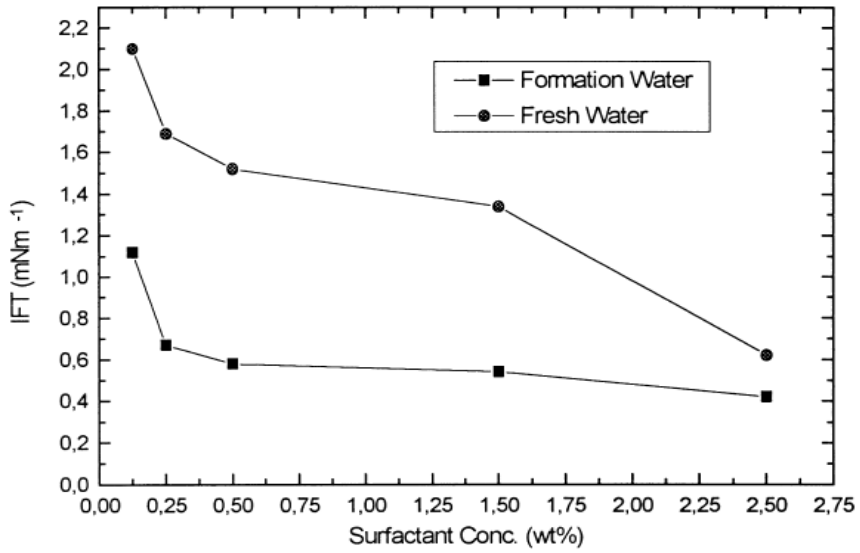

Figure 14: Emulsion viscosity as a function of water salinity at different surfactant concentrations (Ahmed et al., 1999).

Effect of emulsifier concentration

An increasing emulsifier concentration is inversely proportional to droplet size due to lower interfacial tension. This decreases in droplet size induces an increase droplets contacting surface which leads increase in emulsion viscosity (Azodi and Solaimany Nazar, 2013). In Figure 15 emulsifier concentration effect is illustrated from the research of Azodi and Solaimany Nazar in 2013.

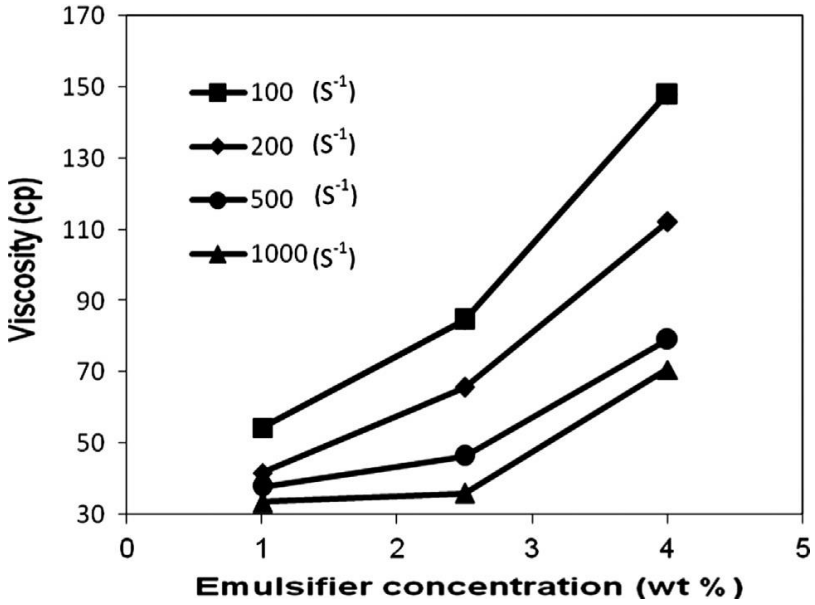

Figure 15: Effect of oil concentration on viscosity of emulsions of oil type 1 at 100, 200, 500 and 1000 (s^{-1}) shear rates (Azodi and Solaimany Nazar, 2013).

Effect of Temperature

The viscosity of oil emulsions are strong function of temperature and decreases with increasing temperature, the main reason is decrease in the viscosity of oil phase.

Ronningsen has introduced correlation for the viscosity of W/O emulsion as a function of the dispersed phase volume fraction and the temperature (Ronningsen). Result of the Roningsen experiment is in figure 16.

$$\ln(\mu_r) = a_1 + a_2T + a_3V + a_4TV \qquad (13)$$

Where, V is volume fraction of dispersed phase, a_1, a_2, a_3 and a_4 are constants, T is temperature, V volume fraction of dispersed phase. "This correlation is based on the exponential relationship between the viscosity and the dispersed phase volume fraction originally suggested by Richardson (1950) and was obtained through an analysis of experimental data of viscosity at different temperature and shear stress" (Farah et al., 2005). Farah *et.al.* tests on w/o emulsion(40% water) in different temperatures is shown in Figure 17.

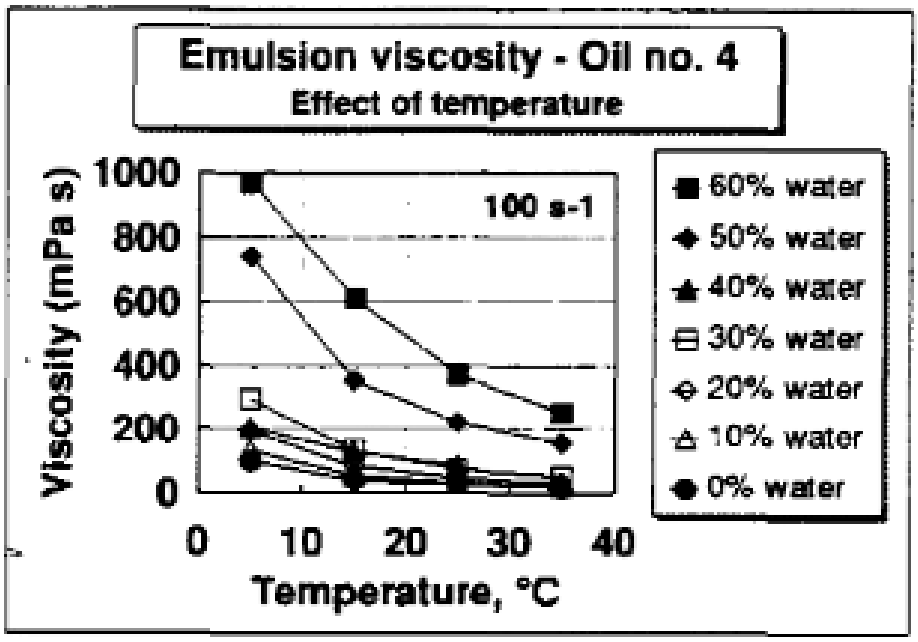

Figure 16: Temperature effect on viscosity of emulsion (Ronningsen, Azodi and Solaimany Nazar, 2013).

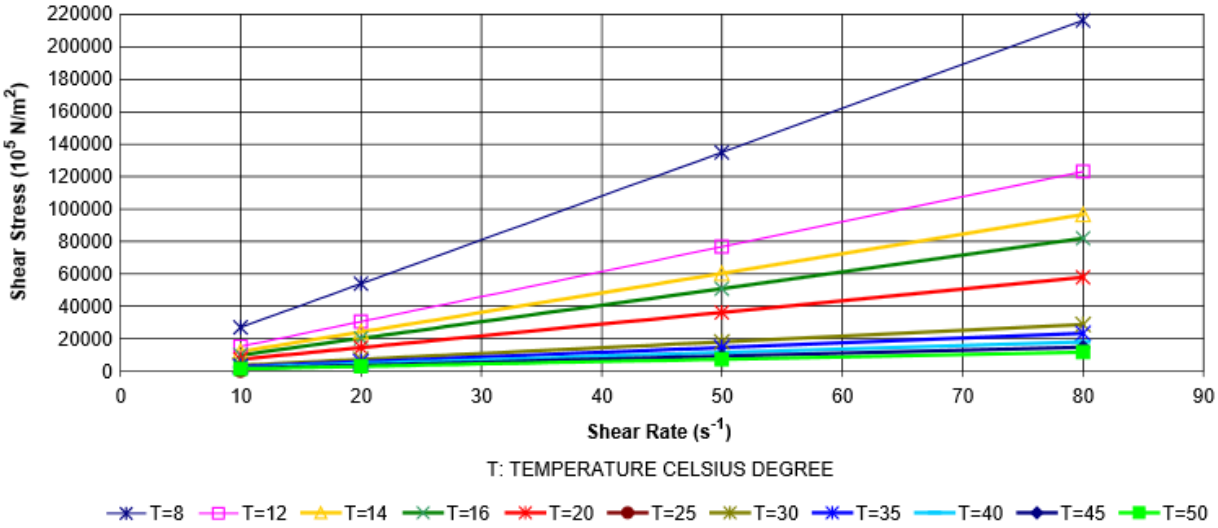

Figure 17: Rheogram at different temperature for fixed volumetric fractions (40% water) (Farah et al., 2005).

3. Experimental setup and procedures

The basic idea was that the ease by which a floating emulsion could be removed would depend on rheological properties, not on chemistry. Thus, if a bio-emulsion can be made with properties similar to a real crude-oil emulsion, the bio-emulsion may be used as substitute in spill recovery tests and exercises. Thus, the approach was to make bio-emulsions, determine their physical and rheological properties and compare these to similar properties measured for a reference crude-oil emulsion.

3.1. Materials

The bio-emulsions were prepared from soy-bean oil (B), emulsifiers(C) and water(A), with salt added. As a natural emulsifier Palsgaard DGMO298™(B1) together with Palsgaard DGPR175™(B2) were used. The compositions of the base emulsion are provided in Table 2.

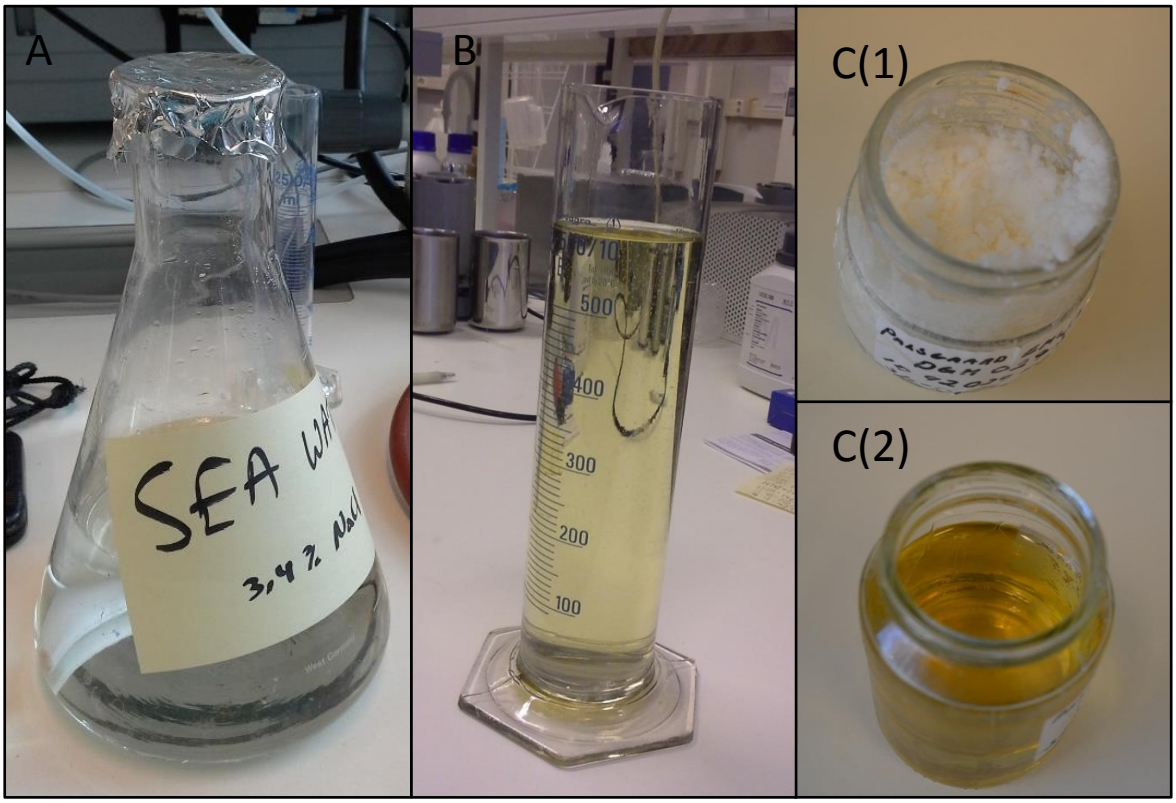

Figure 18: (A)seawater, (B) soybeanoil, C(1) Palsgaard DGMO298™ and C(2) Palsgaard DGPR175™(B2)

Table 2: Composition of the base emulsion.

Ingredient	*Volume %*	*Amount [ml]*
Soybean oil	*29.5*	*118*
Seawater	*69.5*	*278*
DGPR	*0.5*	*2*
DGM	*0.5*	*2*
Total	*100*	*400*

Table 3 below lists the properties of these emulsifiers.

Table 3: Properties of emulsifiers.

Product Type	*Functional Properties*	*Functional Properties*	*Dosage*
Palsgaard ® PGPR 4175 (polyglycerol polyricinoleate (PGPR))	*Used as Water-in-Oil emulsifier for production : - Low fat spread emulsions - Tin greasing emulsions*	*- Has a strong emulsifying effect - Increases the viscosity in emulsions, contributing additionally to the emulsion stability - Reduces the surface tension between the water and the fat phase - Stabilizes the water-in-oil emulsion during the emulsification and cooling - Ensures a stable and homogeneous emulsion in the margarine with a low fat content. - Developed for very low water-in-oil emulsions*	*0.03 % - 0.4% in low fat spread emulsions*
Palsgaard ® DMG 0298 (distilled monoglycerides of vegetable fatty acids)	*- Used for low fat and very low fat margarine*	*- Reduces the surface tension between the water and the fat phase. - Stabilizes the Water-in-Oil emulsion during emulsification and cooling. - Ensures a stable and homogeneous emulsion in margarine with a low fat content. - The fatty acids composition is mainly based on oleic acids*	*0.1% - 0.8 %, calculated on the finished product but no limitation*

3.1.1. Preparation of bio-emulsion

The experiment started by preparing the water phase of the emulsion, the so-called seawater, from 3.4% NaCl and tap water. Then soy bean oil was heated to the 40°C for enable emulsifier to be solved in the oil. Mixing the emulsifier with oil phase at desired condition (T=40°C and Low rotational speed) by IKAMAG RCT, is illustrated in figure 21. After having fully dissolved emulsifiers in oil, water could be mixed to the emulsified oil. The key

point during the mixing of water to emulsified oil is, amount of water should be added during first attempt. Amount of water should not exceed around twenty percentage of water which had been planned to add. If the water is exceeded that limit it will be nearly impossible to mix them anymore with the mixers available. Therefore, the lesser addition of water in each step will make easier for water to make droplets in oil phase which creates emulsion. Then, next added proportions of water should me mixed to get final desired emulsion. With the mixer illustrated (IKAMAG RCT) some segregation of water phase to the bottom of the beaker was experienced. In first steps mixing with hand (by using spoon etc.) could be much more helpful to make small droplets of water suspended in oil phase. Then Another mixer (IKA RW 20 DZM RCT), shown in figure 22(A), could be used to prepare the emulsion at 150-200 rpm rotational speed.

The emulsion samples made, were intended to be water-continuous, checking To make sure that the prepared bio-oil emulsion does not change to Oil-in-Water emulsion, a droplet of the emulsion was placed on a clear water surface and visual inspection was done to see whether emulsion is solved in water or not. If any dissolving happens it could be explained as the emulsion or some portion of emulsion is changed to Oil-in-Water from Water-in-Oil emulsion. The mixing of emulsion in very high rotational speed is a potential reason for that change. As it is shown in figure 19, the droplet was not dissolved in water.

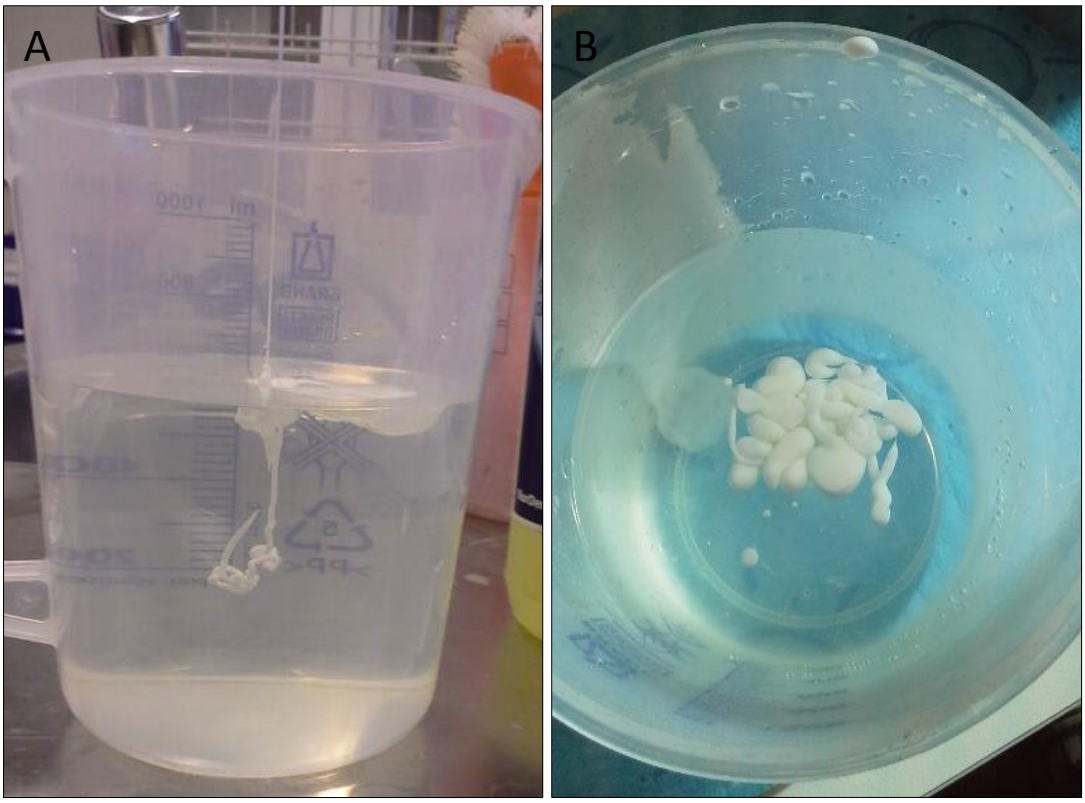

Figure 19: Prepared emulsion – drop into the water.

3.1.2. Crude-Oil Reference Emulsion

Crude-oil emulsions are found in many forms, depending on the chemical composition of the crude and the weathering it has been subjected to. For the current investigation an emulsion specially designed and prepared for the previously mentioned Oil-on-Water exercise was used NOFO. The design criterion was that it should be representative for emulsions resulting from crude oil release in the Halten-area, offshore Norway. The emulsion was provided by S. Ramstad, SINTEF, and prepared from light North Sea Crude (Oseberg Blend), stripped by evaporation at 200°C, with addition of heavy oil and mixing with sea water. This provided a relatively consistent and stable, oil-continuous emulsion with water content around 70%. Figure 3 below shows this emulsion. The crude oil emulsion was also tested in order to see the is emulsion W-O or O-W. As it can be observed emulsion is W-O as prepared bio-emulsion.

Figure 20: Crude-oil emulsion (A) crude oil emulsion sample, (B) drop of crude oil emulsion into water to check the type of emulsion.

3.2. Measurements, apparatus and procedures

3.2.1. Anton Paar Viscometer

Any type or combination of rheological tests, both in rotational and oscillatory mode and temperature variation are possible with the MCR Anton Paar viscometer. In addition, the viscometer has wide range capacity to do rheological tests for desired temperature. By using integrated devices, temperature can range between -150°C to 1000°C. The equipment has different additional accessories which can be used for extended material characterization; The purpose of using Anton Paar viscometer in this experiment is, to have very precise investigation dynamic viscosity of the assortment of emulsions in different temperatures.

3.2.2. IKAMAG RCT

The apparatus have ability to heat-up the fluid up to 500 C° and can mix fluid by using rotational magnetic plate which drives other cylindrical spare magnet inside the fluid(see

figure 21). Rotational speed and heating ability is more than enough to mix the emulsifier with oil phase at desired condition (T=40 C° and Low rotational speed).

Only limitation of the IKAMAG RCT(figure 21) for this experiment is not being capable of mixing oil phase with water to make an emulsion. When the water phase added to emulsion it segregates to the bottom of the cup and even one hour mixing could not crate the emulsion. Most probably, it is happening due to the cylindrical shape of the magnet which could not break the water phase to the small water bubbles.

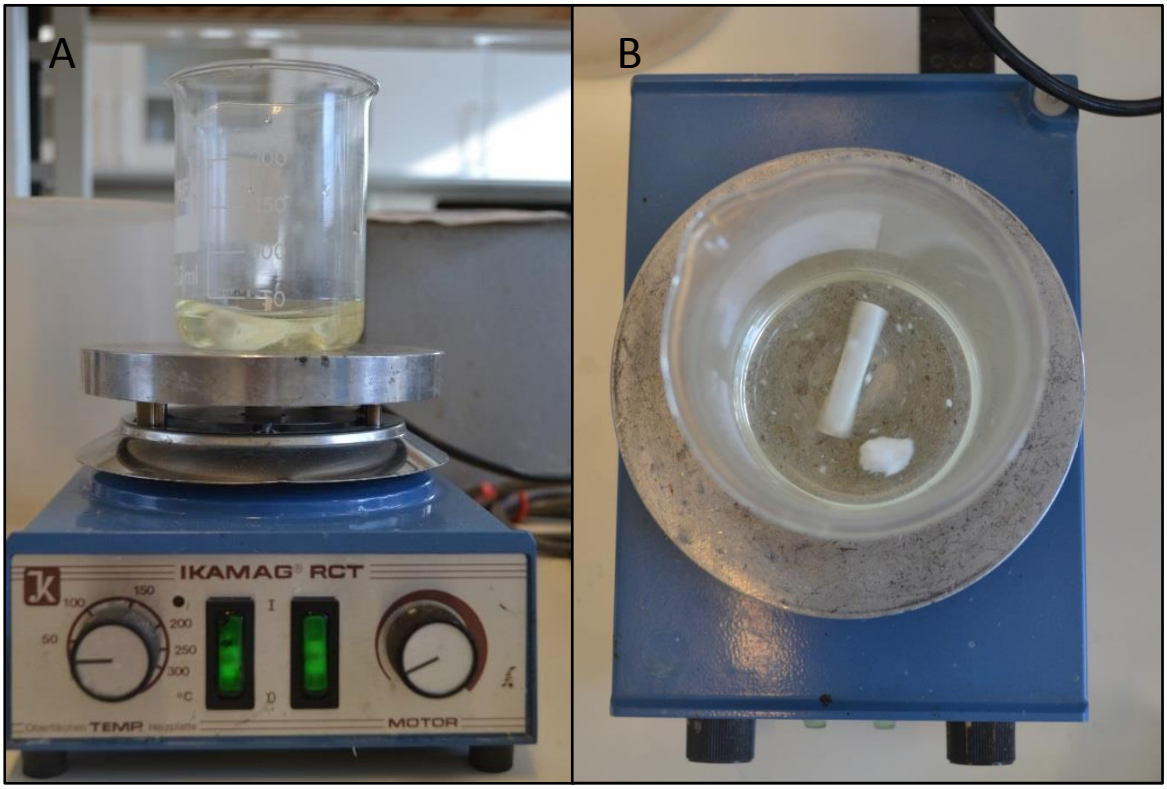

Figure 21:IKAMAG RCT, (A) front view and (B) top view.

3.2.3. IKA RW 20 DZM RCT

IKA RW 20 DZM RCT is a mixer which can be adjusted for specific rotation speeds. Mixing speed to prepare emulsion is limited with high range which should not exceed 200 rpm not to break emulsion. Due to the limitations of IKAMAG RCT(see above), mixing with IKA RW 20 DZM RCT and hand is the appropriate methods to have preferred emulsion properties. However, duration of using mixer is also limited with excessive heating of equipment motor. Mixing with hand (tea spoon etc.) would be much more efficient for the period of the beginning of the mixing water with emulsified oil to prepare emulsion. Then mixer could be used to have more stable emulsion with smaller droplet sizes.

3.2.4. Axio Imager 2 from Carl Zeiss

The microscope Axio Imager 2 from Carl Zeiss(see figure 22B) is used for taking the pictures of emulsion which can help to detect the droplet sizes emulsions. The microscope belongs to the Department of Biology of NTNU which can provide very accurate digital images in the desired range (10-50 µm) for the emulsion samples. Microscopic pictures of emulsion samples are taken by adjusting the lighting in order to avoid blurred images(see figure 23). Moreover, blue colour which could solved in water phase only was added to the emulsion for making colour difference between soya oil and water which is resulted better image processing.

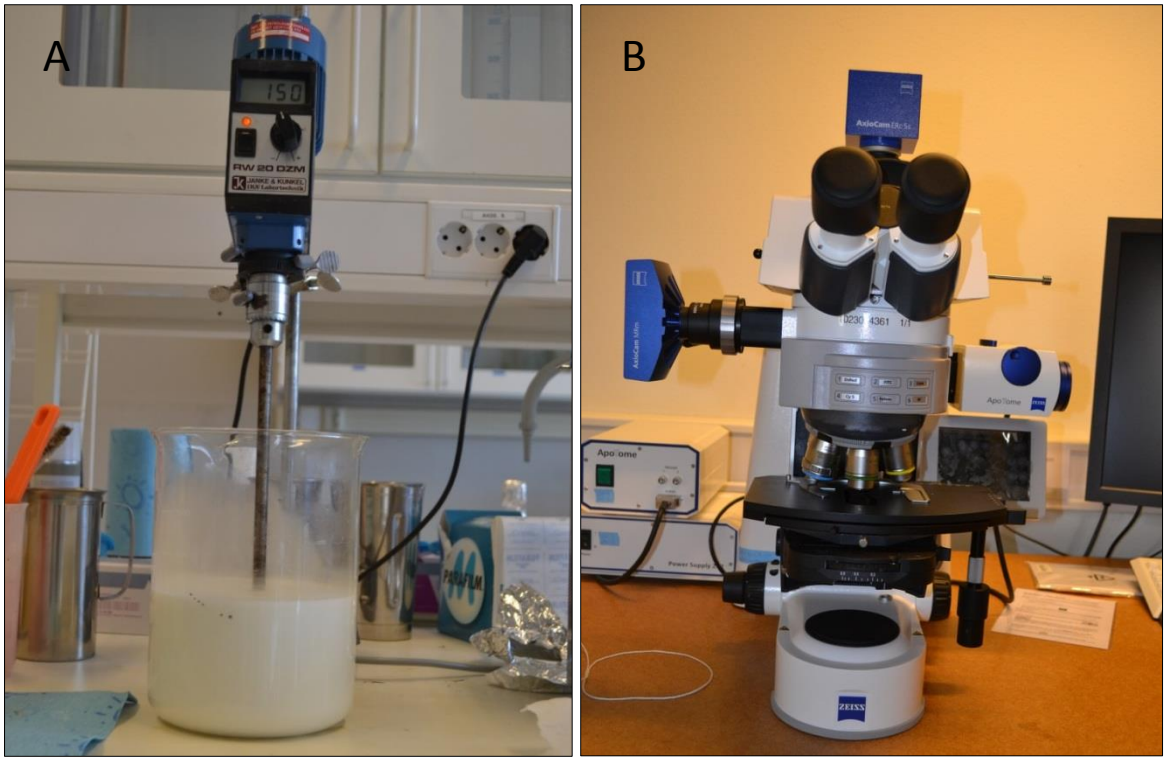

Figure 22: IKAMAG RCT mixer(A) and microscope Axio Imager 2 from Carl Zeiss(B)

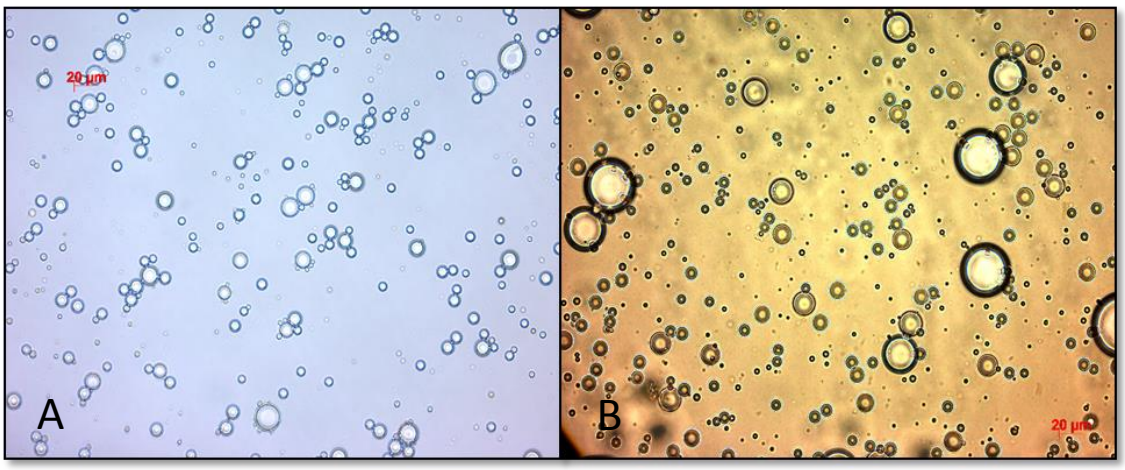

Figure 23: Microscopic image of bio-oil (A) and crude-oil (B) emulsion.

3.3. ImageJ software

"ImageJ is a free image processing and analysis program that can be utilized to develop user-coded plugins to suit the specific requirements of any conceived application. ImageJ is a Java-based public domain image processing and analysis program developed at the National Institutes of Health (NIH), USA, which is freely available, open source, multithreaded and platform independent with tools for user-coded macro and plugin development developed an ImageJ plugin to determine the dimensions of singulated particles by identifying their shapes and analyze their size distribution" (Igathinathane, Pordesimo, Columbus, Batchelor, & Sokhansanj, 2009).

For this experiment the software assisted to process the microscopic images of the emulsion for analyzing water bubbles on images as it is shown the figure 25. Image is processed with the software to find the area and Feret's diameter of the bubbles. Feret's diameter can be defined as "distance between two parallel tangets on opposite side of the image randomly oriented particle (sometimes, the average value over many orientations is used)" (Merkus, 2009) it is also known as maximum caliper. The angle (0–180 degrees) of the Feret's diameter is displayed as FeretAngle, as well as the minimum caliper diameter
The starting coordinates of the Feret diameter (FeretX and FeretY) are also displayed. There are different approaches for determining the particle sizes figure 24 below shows the method of determining the projected particle sizes(Arai, 1996).

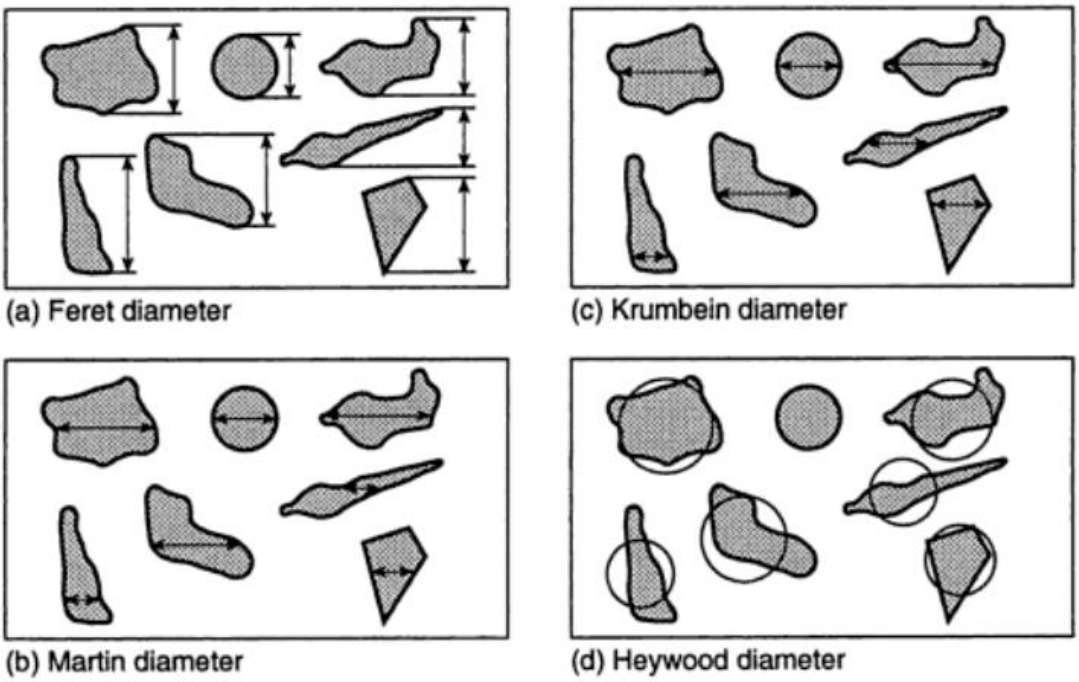

Figure 24: Measurement of particle diameter with different methods(Arai, 1996).

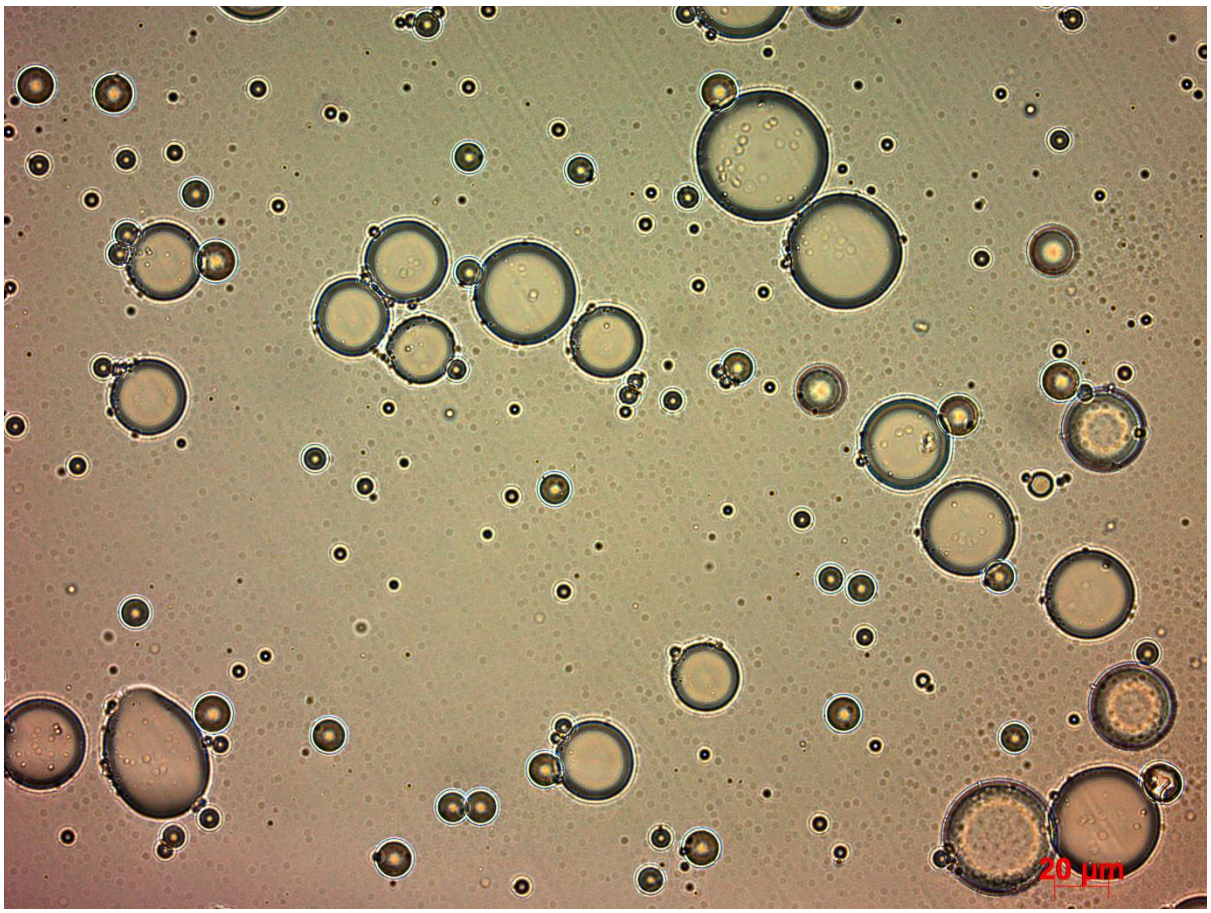

Figure 25: Microscopic image of the bio-emulsion (no color added)

The processing of images starts by converting actual images to binary images before being processed by the application algorithm. The figure below is raw binary image of the microscopic picture without any modification (brightness adjustment). As it is shown from the figure binary image has noise on it. Therefore, it is helpful to adjust brightness and colour of the images in order to avoid the noise (dark part of the pictures which can be observed on the top left side of the figure 26)

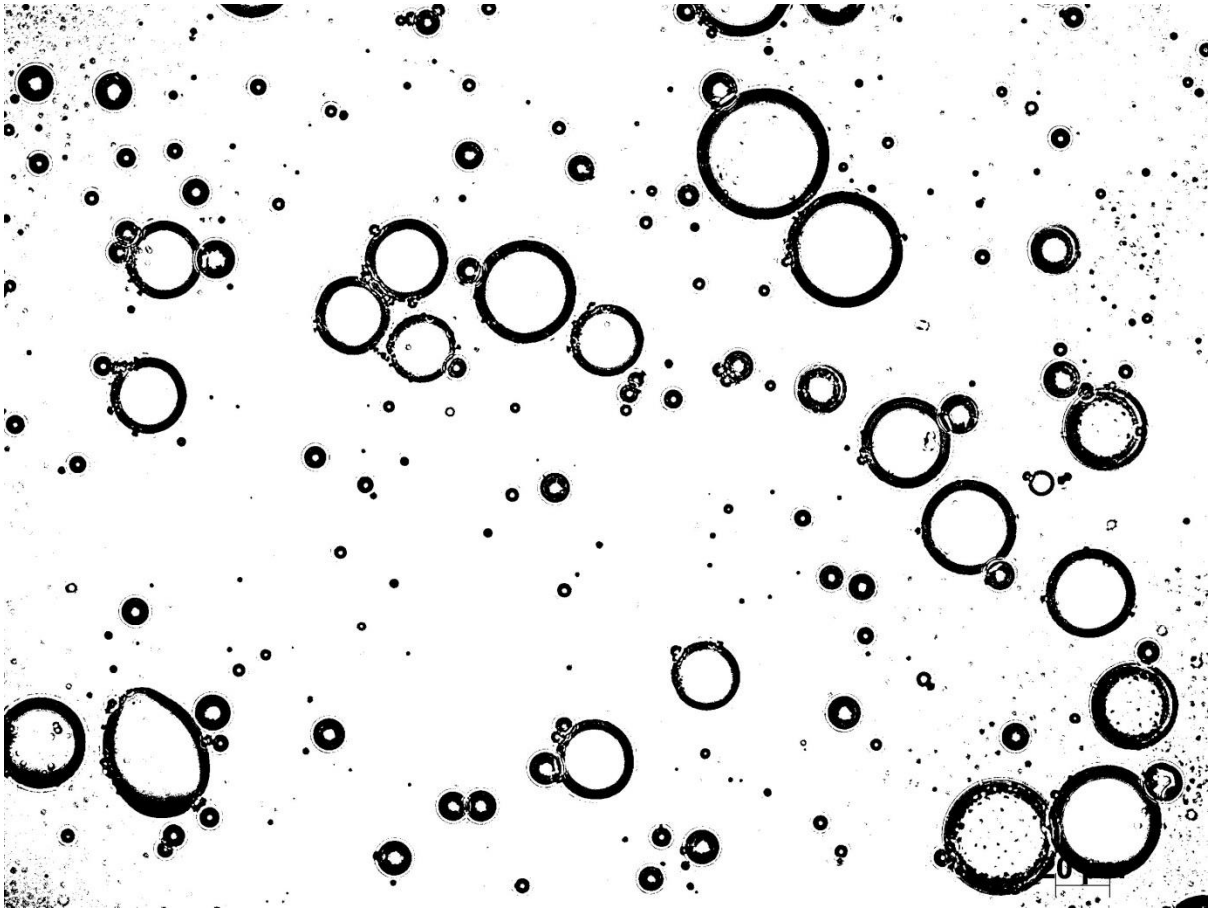

Figure 26: Raw binary image of the microscopic picture without any modification

The figure 26 is binary image of microscopic picture where colour is adjusted before changing it to the binary. ImageJ has a function to "fill the holes" which is applied to the image shows the result. After filling the holes some bubbles still can show without filled; in this case pencil tool is used to close the gaps on the border of circle in order to help software to detect them as a full circle and be able to fill the holes. After having the fully filled

bubbles, a function on ImageJ called “Watershed” applied to image which is capable of identifying the edge of adjacent water droplets.

After separation, the binary image was manually compared with the original image for consistency and correct binary conversion. Droplets not separated by watershedding were corrected using the ImageJ pencil tool. The Figure27 is processed version of the binary picture where all holes are filled and split. As the purpose of image processing is to find the particle distribution and averaged parameters (such as diameter and volume) of the water droplets in oil, these steps are very important for not missing any bubble that have impact on averaging.

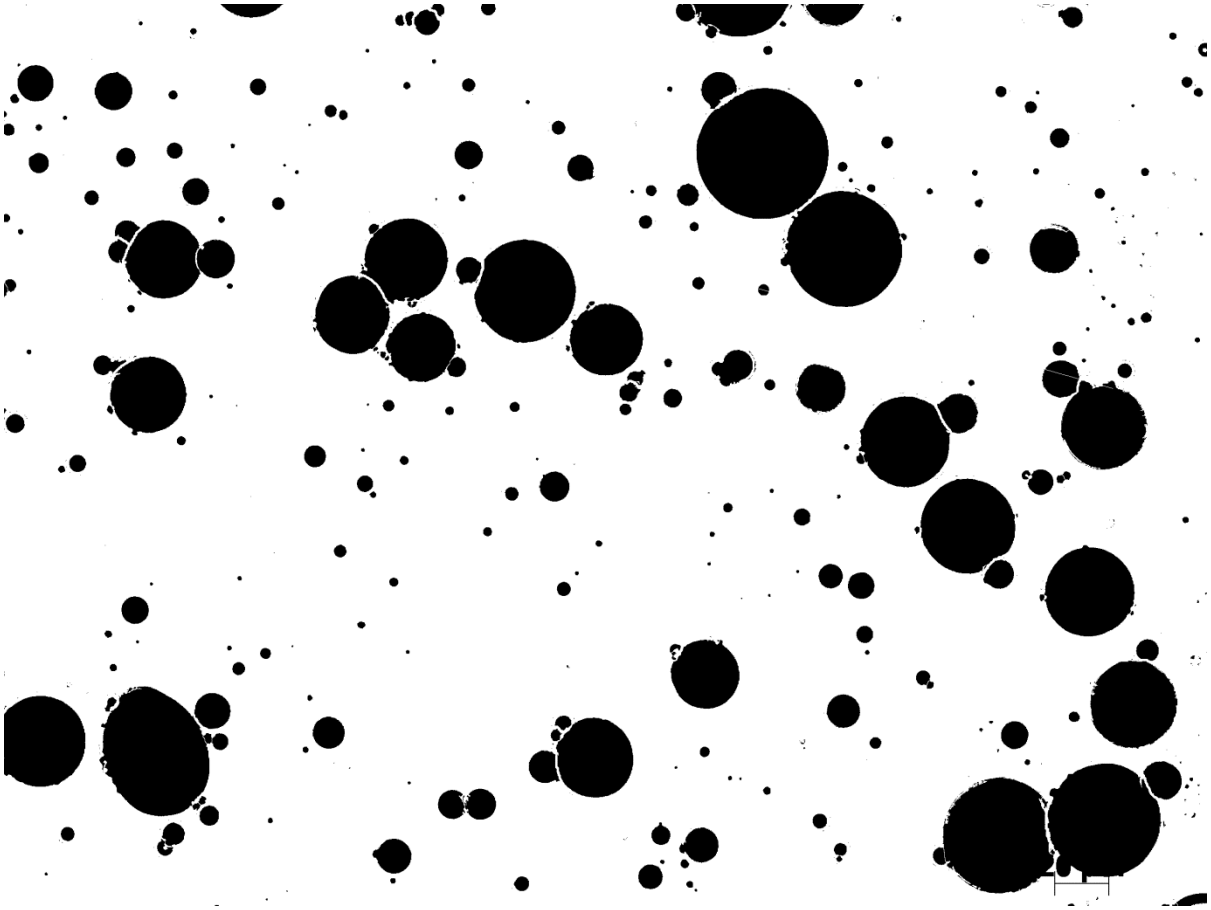

Figure 27: Processed version of the binary picture where all holes are filled and split

After making all adjustment on the picture scale needed to input to the software. As it is shown the figure 25 microscope has a function to add scale on the images (see right bottom of the figure). Proper calibration of image is essential for the parameter calculation is required. The calibration procedure basically defines a scale factor, which converts the pixel units of the image to physical units of dimensions (Igathinathane et al., 2009). Then, the area and the diameter of the droplets are displayed in micrometres by ImageJ. Now, Area and

Feret's diameter should be selected from the available parameters in the set measurement option. In this case the result is calculated by using "Analyse Particles" option. ImageJ calculates area and Feret's diameter (including average, minimum and maximum) and exports it to a Microsoft Excel format (.xls). In addition, results are displayed in the figure below.

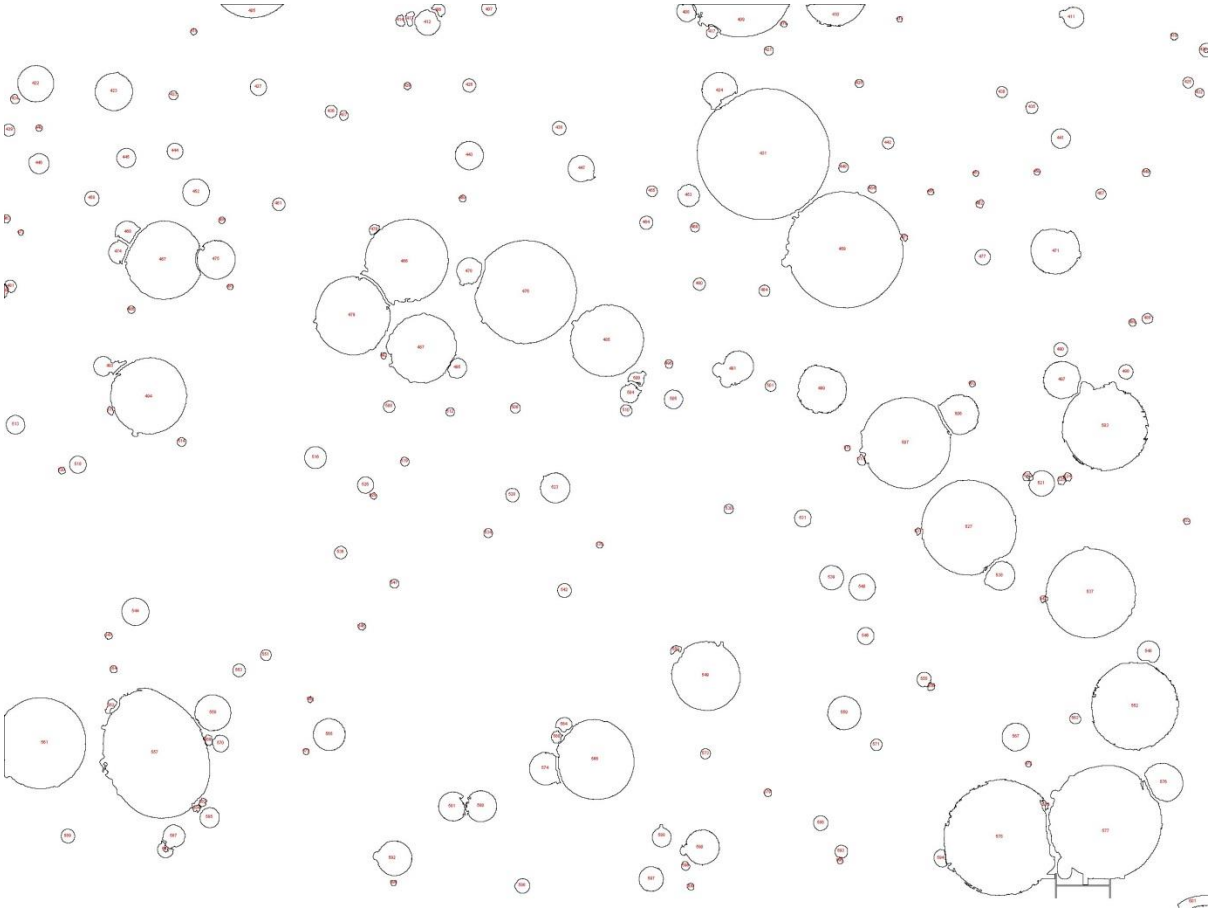

Figure 28: Measured water droplets and each particle is numbered

Exported results from ImageJ is analyzed by using MATLAB software. MATLAB code is provided by my supervisor prof H.A.Asheim which could be found on Appendix.

4. Result and Discussion

4.1. Aging

The stability of petroleum emulsions is significantly related to the aging(Malassagne-Bulgarelli and McGrath, 2013) . In 2012, Filho et al. showed that petroleum emulsions are even more affected by aging than concentration of asphaltene, the main emulsifier in crude-oil emulsions(Maia Filho et al., 2012).

In our experiment, bio-oil emulsion started to destabilize after four months of holding it in the laboratory (figure 29 A) Blue color added to water phase in order to see clearly observe the phase difference. This happened even in shorter period for the crude oil samples, approximately two weeks (figure 29 B).

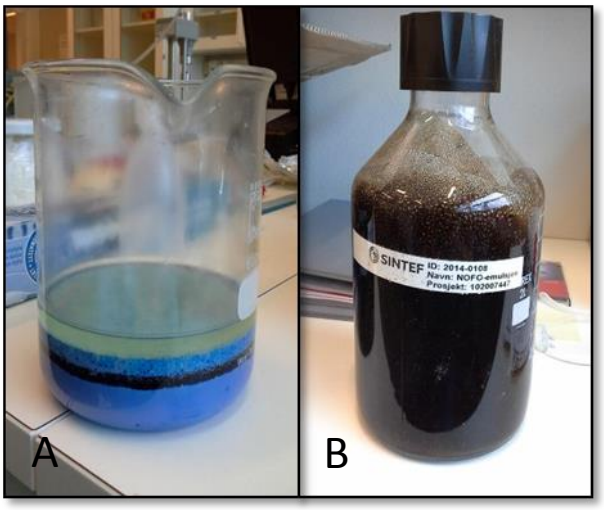

Figure 29: Aged bio-oil (A) and crude oil (B) emulsion.

In the emulsion, the droplets and films apparently form a lattice with significant restriction to geometry change, manifested by high effective viscosity. Fig. 8 illustrates shear tension measured at 20°C, for different shear rates for both crude-oil and bio-oil emulsions.

4.2. Rheology variation and comparison

Rheology of both emulsion are studied in order to find out the both, bio-emulsion and crude oil emulsion rheology and show the similarity between them.

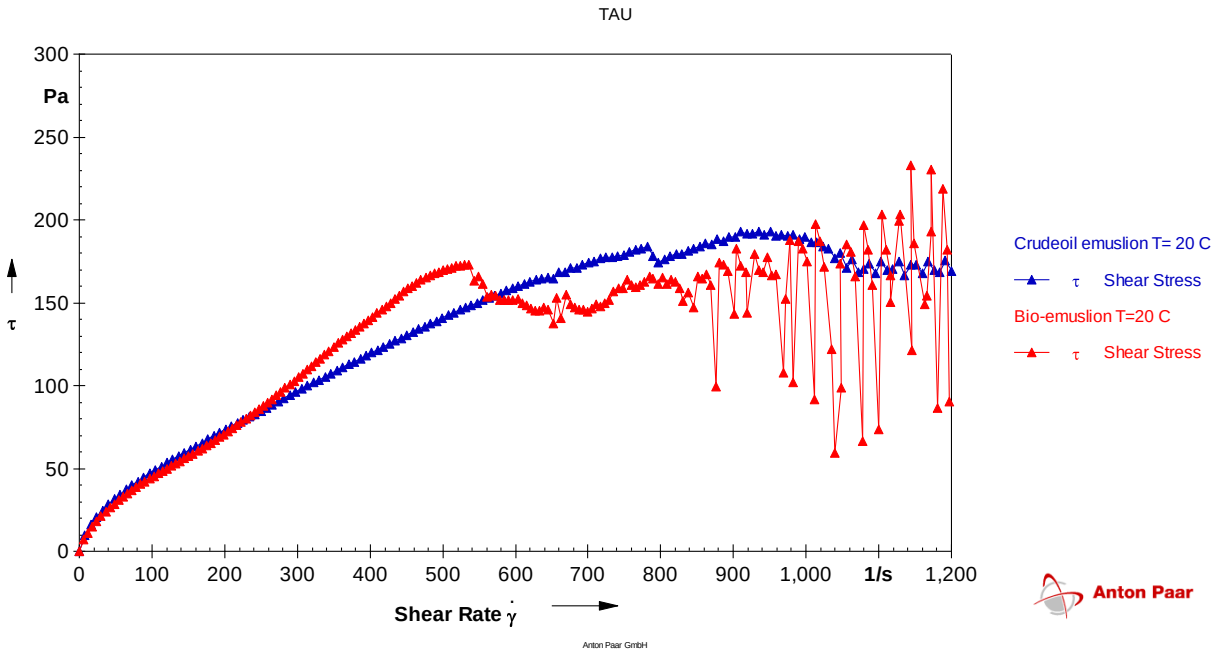

Figure 30: Shear stress/shear rate relationship for crude-oil and bio-oil emulsions.

Fig. 30 shows that except for the high shear rate, the measured shear stresses fit very well to the common power-law relation.

At high shear rates, approximately 500 s^{-1} for bio-oil emulsion, and 800 s^{-1} for crude-oil emulsion, a drastic change in the trend of plots occur. This is likely due to break down of the emulsion lattice, providing free water. According to Princen, both emulsions and foams can be destroyed when subjected to sufficiently high shear rate(Princen, 1983).

Mixing time of the emulsion was investigated in the experiment in order to find the impact of the mixing duration on the dynamic viscosity of the emulsion. In order to investigate the impact of mixing, prepared base bio-emulsion sample (70% water, 30 soybean oil and 1% emulsifier) is compared to the same emulsion but 30 and 45 minute further mixed. The figure 31 below shows the result of dynamic viscosity of the emulsion in different shear rates. As it is shown from the figure more mixing time has increased the viscosity of the emulsion which could be explained as more mixing caused droplets become smaller than the base case which is increasing the viscosity of the emulsion. However, if emulsion is kept for

rest, creaming and sedimentation might occur among the created smaller droplets by increased mixing time.

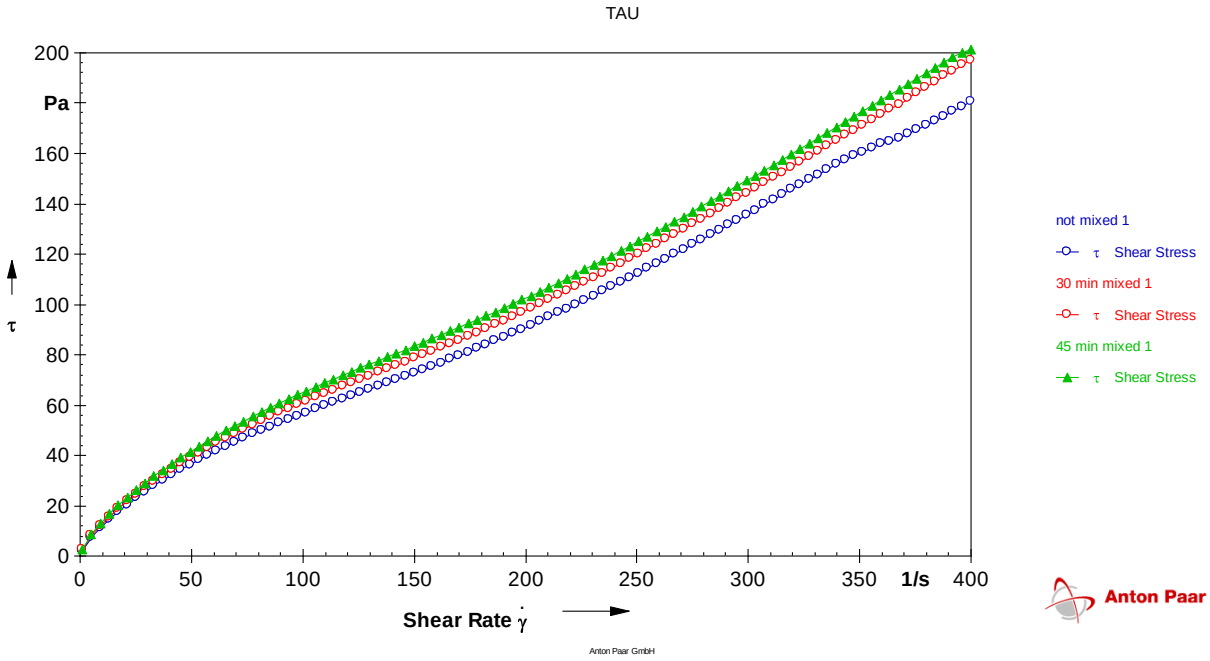

Figure 31 Shear stress/shear rate relationship of bio-emulsion for different mixing time

Therefore, during the preparation of emulsion for different sensitivities such as in case of varied temperature experiment mixing time and the rpm of mixer were kept same in order to have accurate results.

Another important factor affecting rheology of emulsion is emulsifier concentration. Higher concentration of emulsion will make smaller water droplets in oil due the more emulsifying agent creates a film over more droplets, which repel each other.

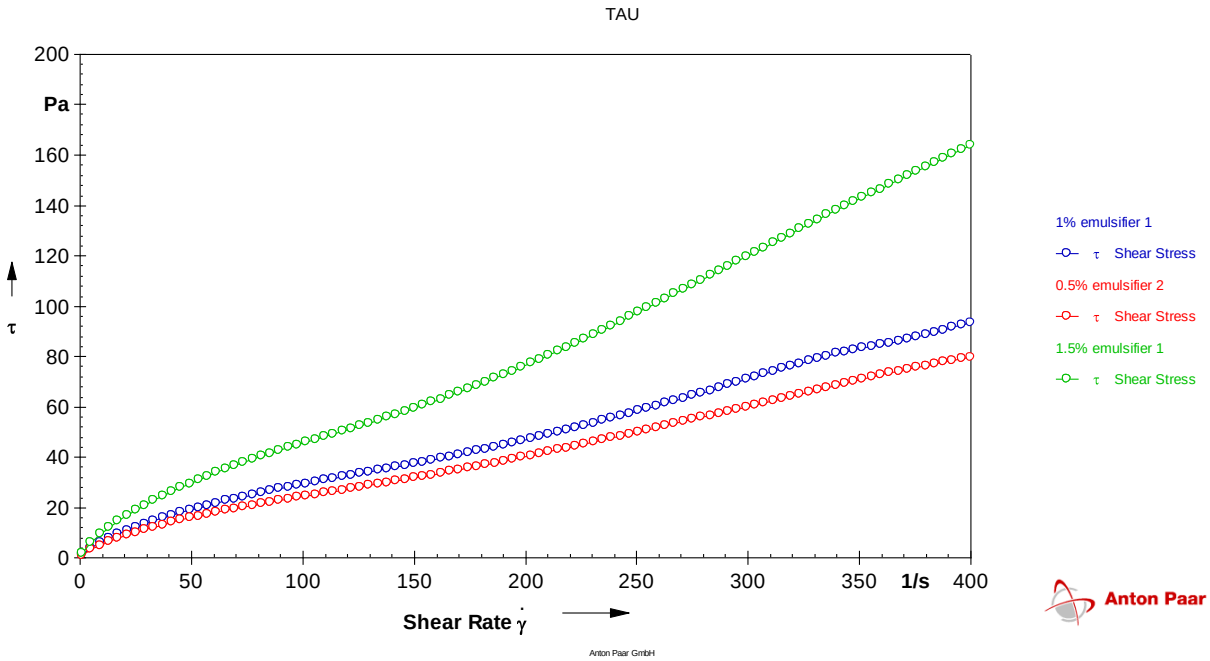

Figure 32: Shear stress/shear rate relationship of bio-emulsion for different emulsifier concentration.

Moreover, impact of salt concentration on the viscosity of the emulsion is also studied in the experiment. The figure 33 shows that the small salt concentration does not have significant impact on the bio-emulsion rheology. Interestingly, according to the Ashrafizadeh *et.al.*, 2012 emulsion viscosity is supposed to increase with an increasing salt concentration for O-W. As the bio-emulsion is W-O therefore and in the experiment water salinity sensitivity was done which is dispersed phase and does not have significant impact on the rheology of the emulsion.

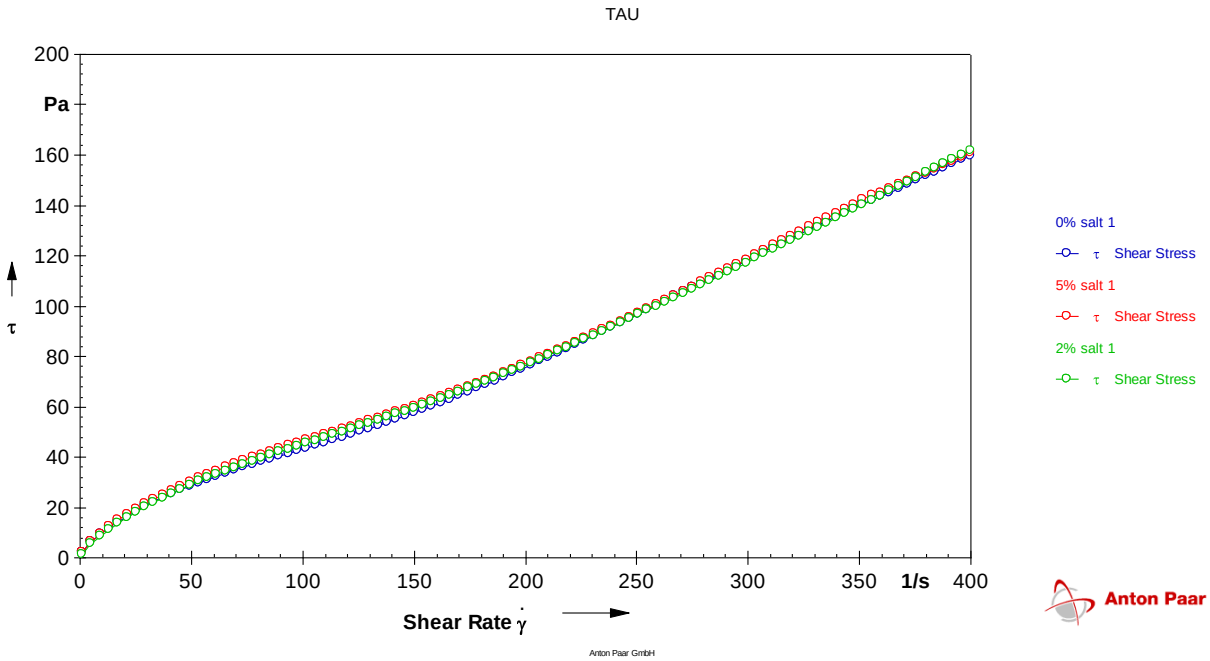

Figure 33: Shear stress/shear rate relationship of bio-emulsion for different salt concentration.

The viscosity of oil emulsions is inversely proportional to temperature(Azodi and Solaimany Nazar, 2013). Shear stress vs. shear rate plot for both bio-emulsion and crude-oil emulsion at different temperatures is shown in the figure 34 below. The almost identical rheological behavior of the two emulsions at 15°C confirms the suitability of substituting crude-oil emulsion with bio-oil emulsion.

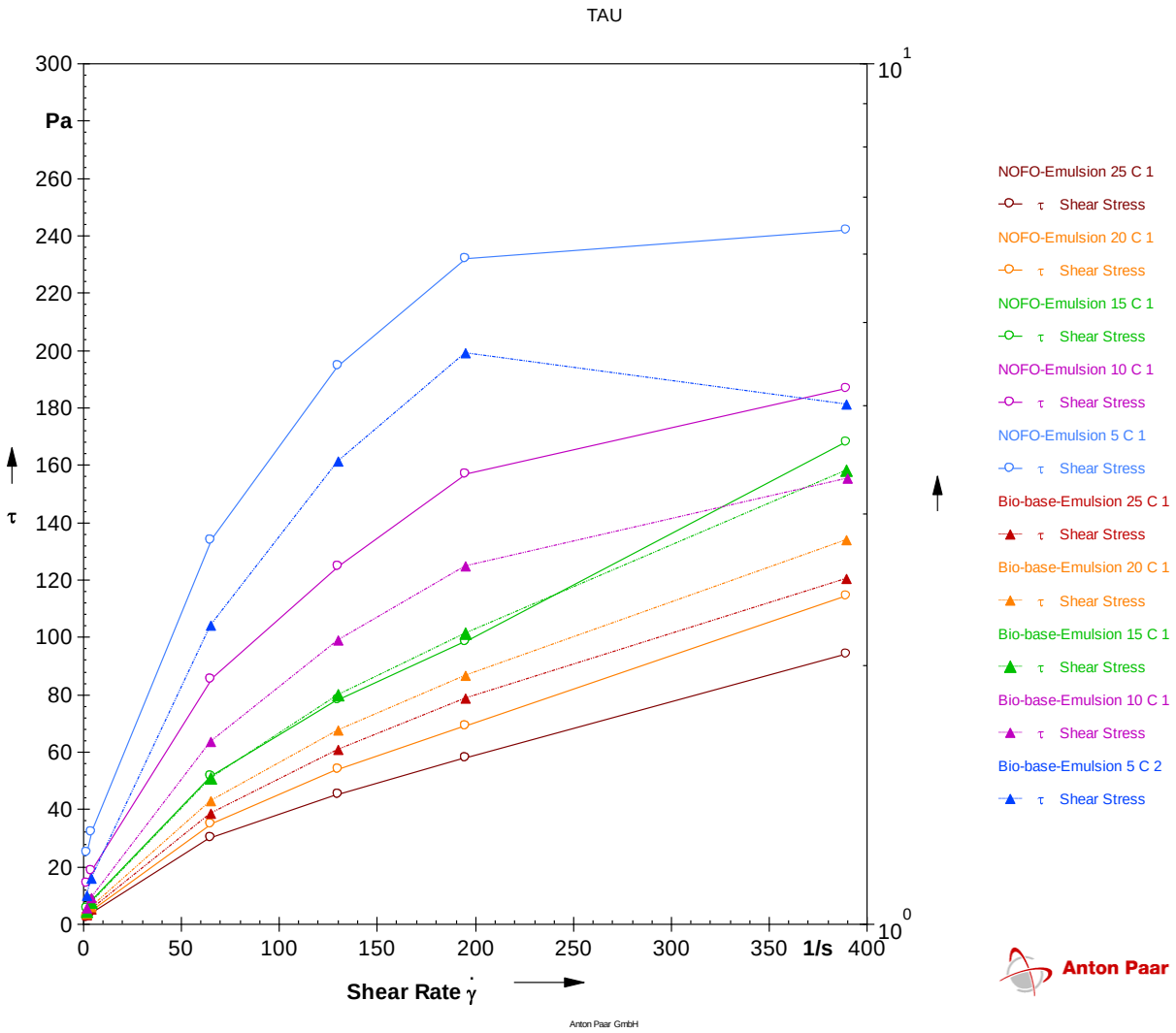

Figure 34: Rheogram at different temperatures for bio-oil emulsion and crude-oil emulsion

For the temperatures below 10°C, the measured stresses are deviating from power-law. In other word $\tau - \tau_{gel} > 0$ which fits to Herschel-Bulkey model which shows that the gel strength of crude-oil emulsion is higher than bio-emulsion.

In the case of given or desired temperature, the rheology of both emulsions could match by altering the bio-emulsion water content or emulsifier concentration.

In the figure 36 bio-emulsion shear stress/shear rate behavior based on bio-emulsion water content is illustrated. Higher the water content is causing higher viscosity because of the more droplets added to the system.

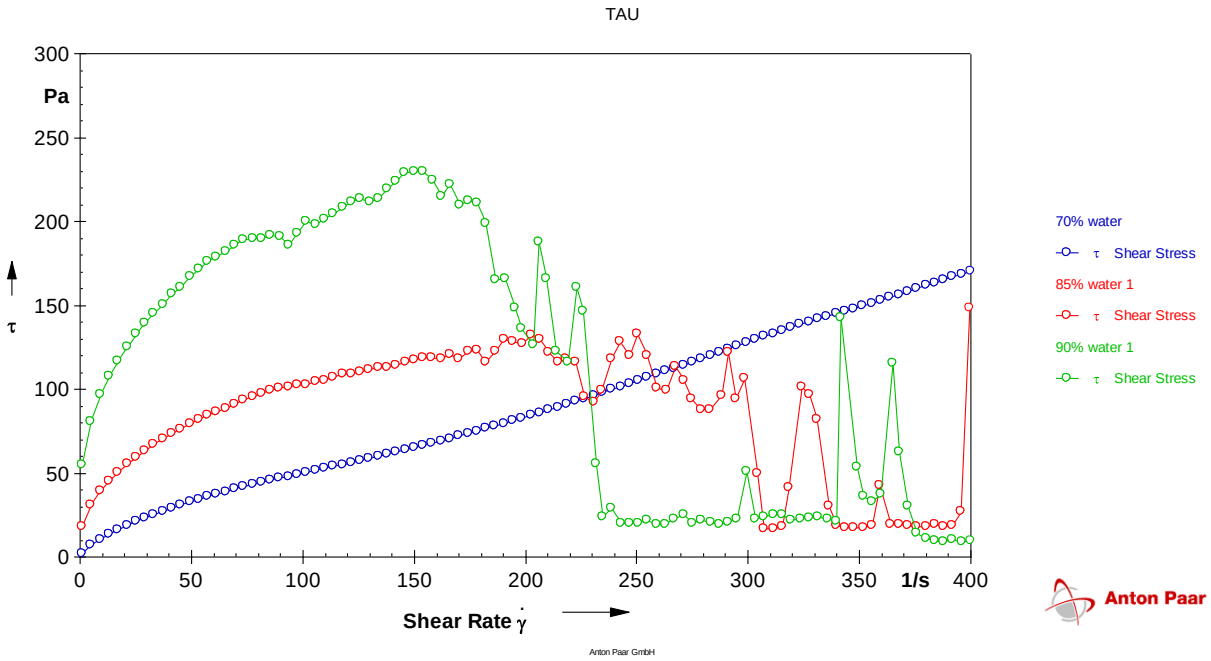

Figure 35: Rheological behavior of bio-emulsion for different water-phase contents and mixing time.

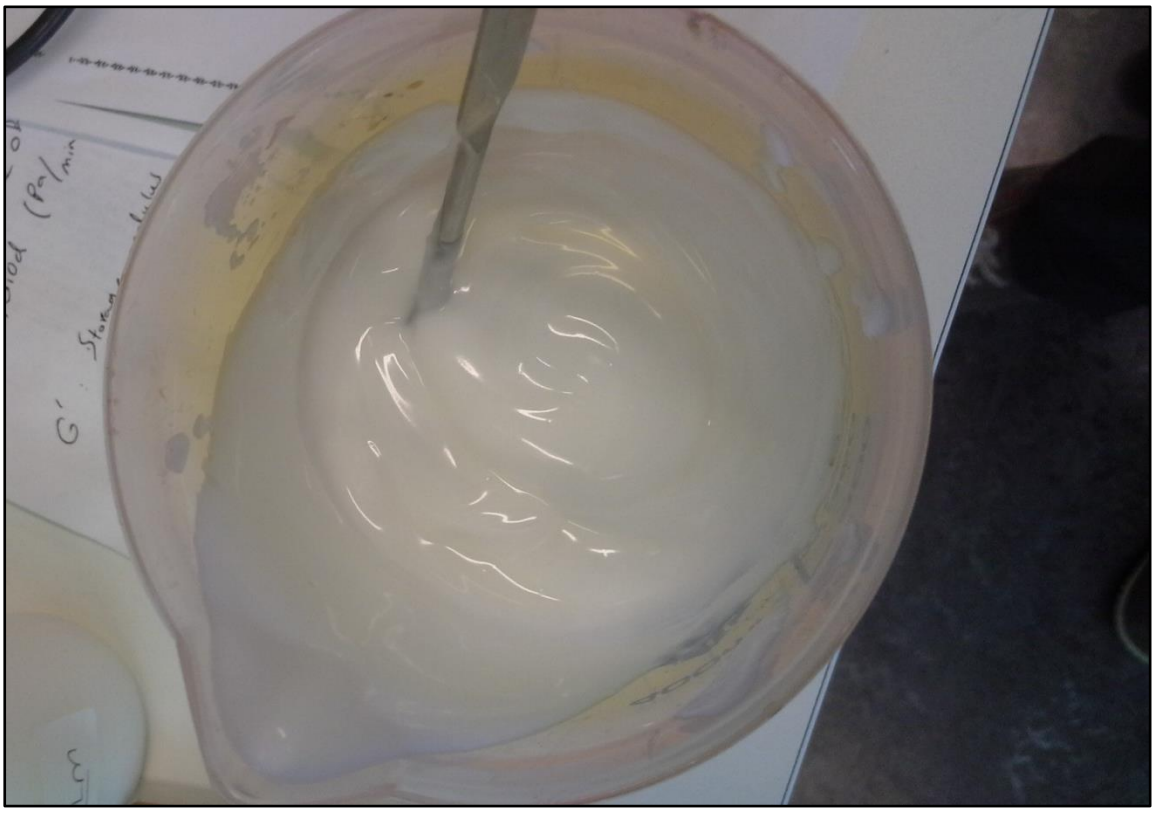

Figure 36: Bio-emulsion has 90% water concentration

4.3. Droplet size comparison

Droplet size has a dramatic influence on emulsion rheology(Pal, 1996). Bio-oil emulsion (see figure 37) and crude oil emulsions (see figure 38) droplet size were studied in this experiment to detect if the results are matching. As it is discussed on the section ImageJ microscopic pictures are analyzed and the results are exported to the excel spreadsheet(see Appendix B for more figures). Then MATLAB software is used to find the average diameter of the droplets on both images.

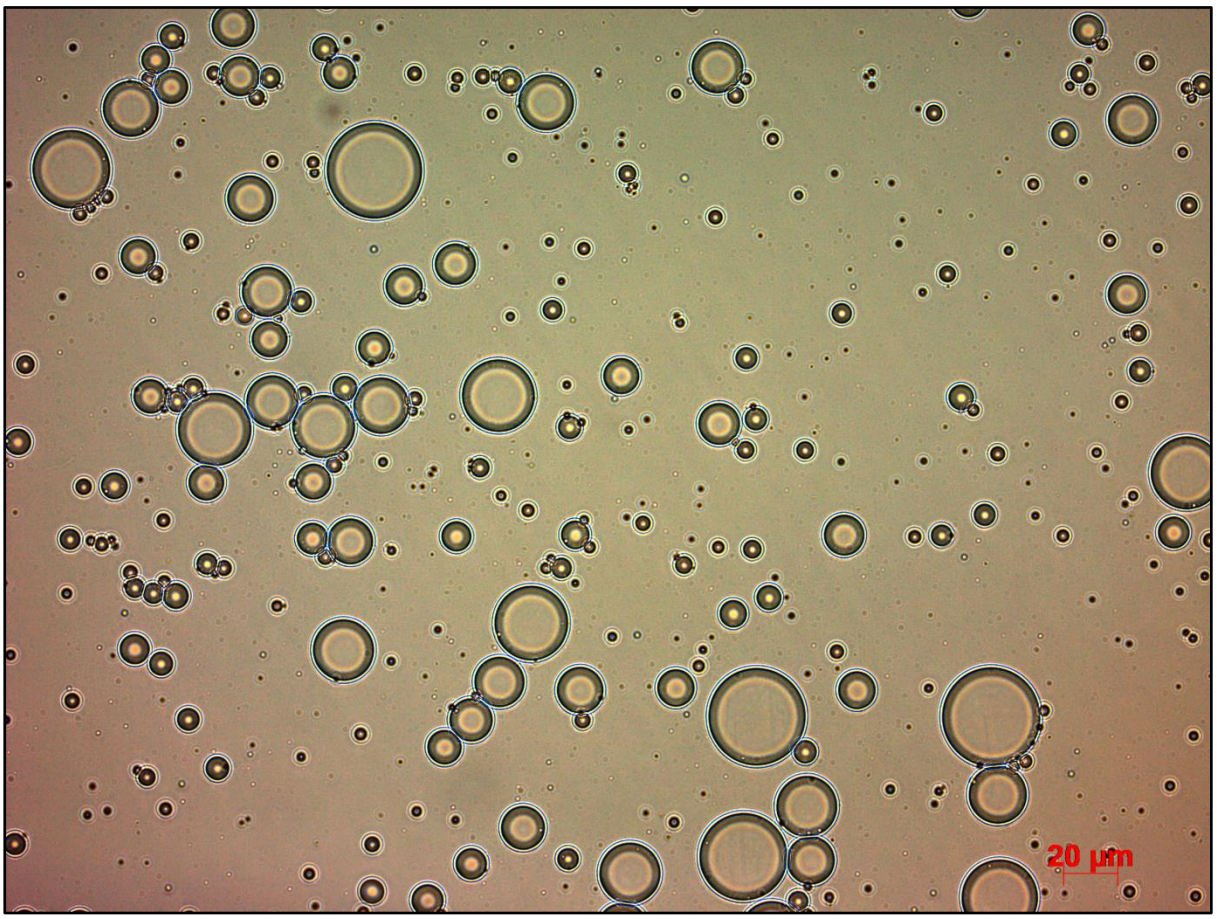

Figure 37: Raw microscopic picture of the base bio-emulsion

The Matlab code calculates average volume for droplets by using Feret(min) and Feret's diameter. It multiplies are found from Feret diameter (which is the biggest possible diameter for each drop) to Feret(min) to find the volume. Then droplet diameter is back calculated by using the formula volume of sphere. Then all results are sorted in the plot.

It can be seen that both emulsions averaged droplet sizes are close each other. It is nearly between in the range of 20-30 µm.

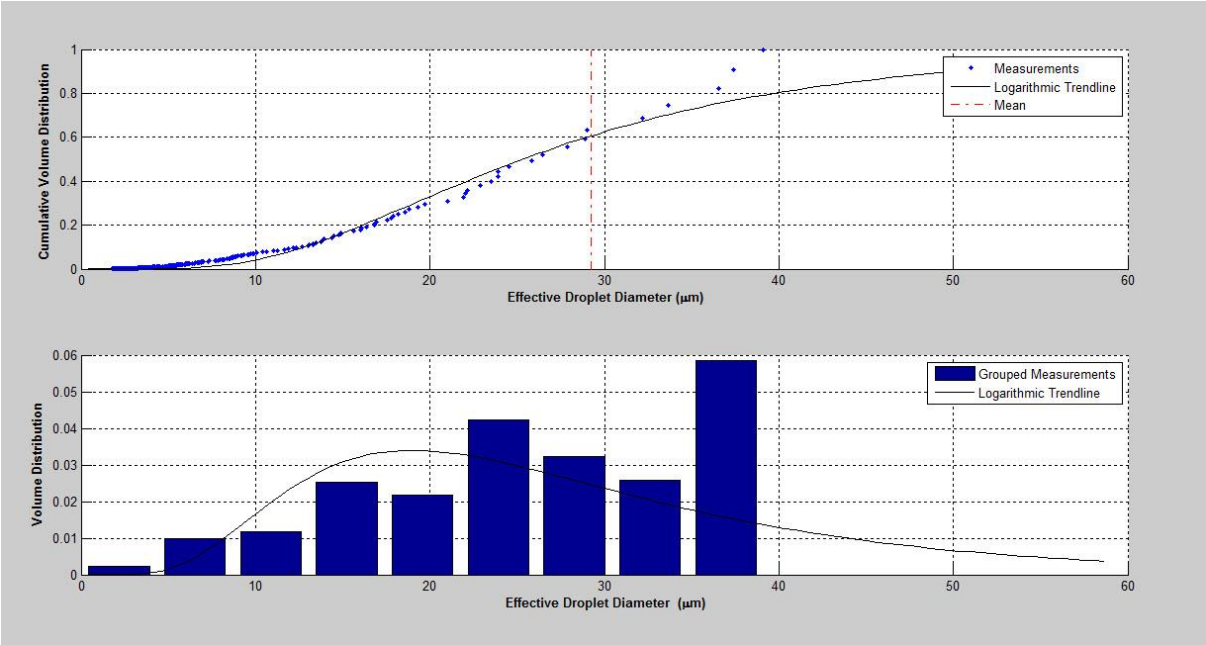

Figure 38: Average droplet diameter for bio-oil emulsion

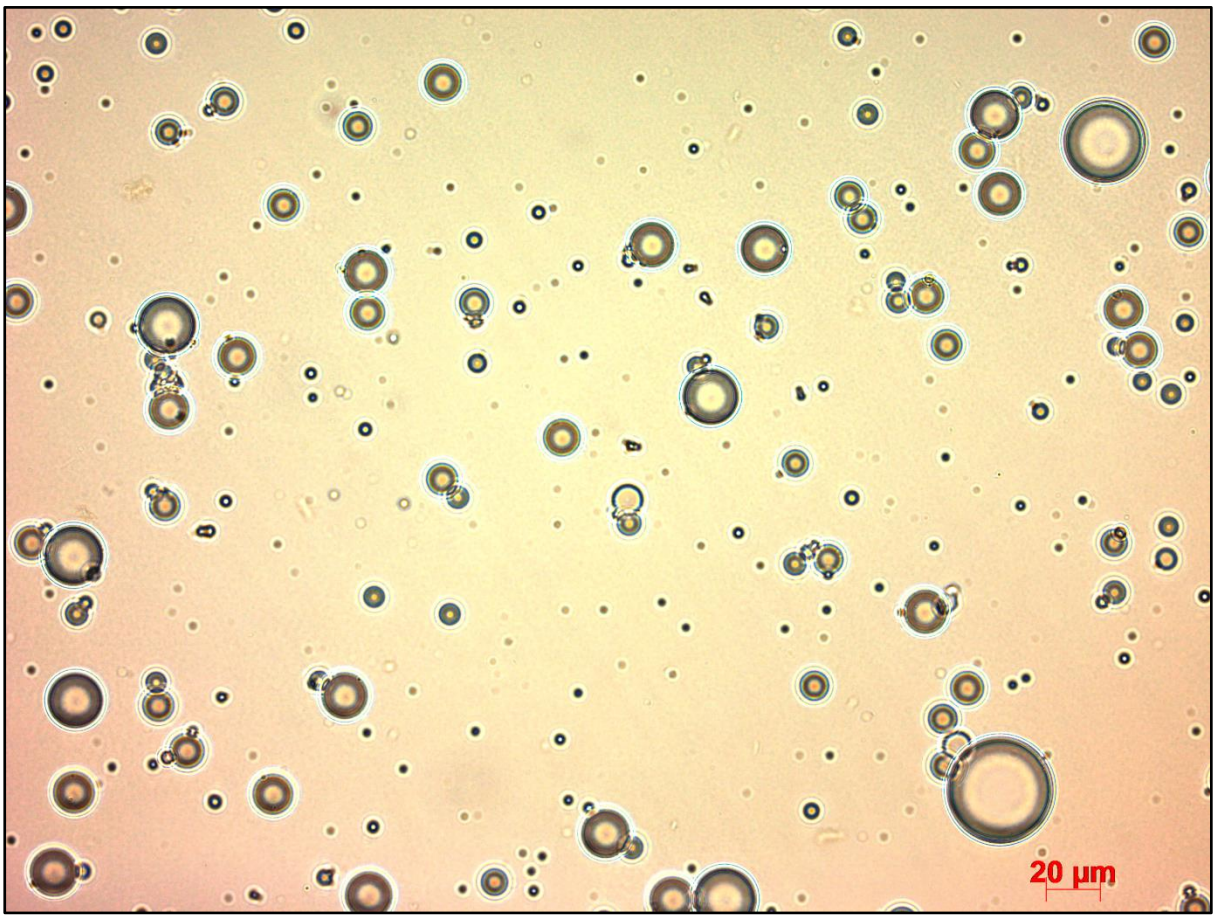

Figure 39: Raw microscopic picture of crude oil emulsion

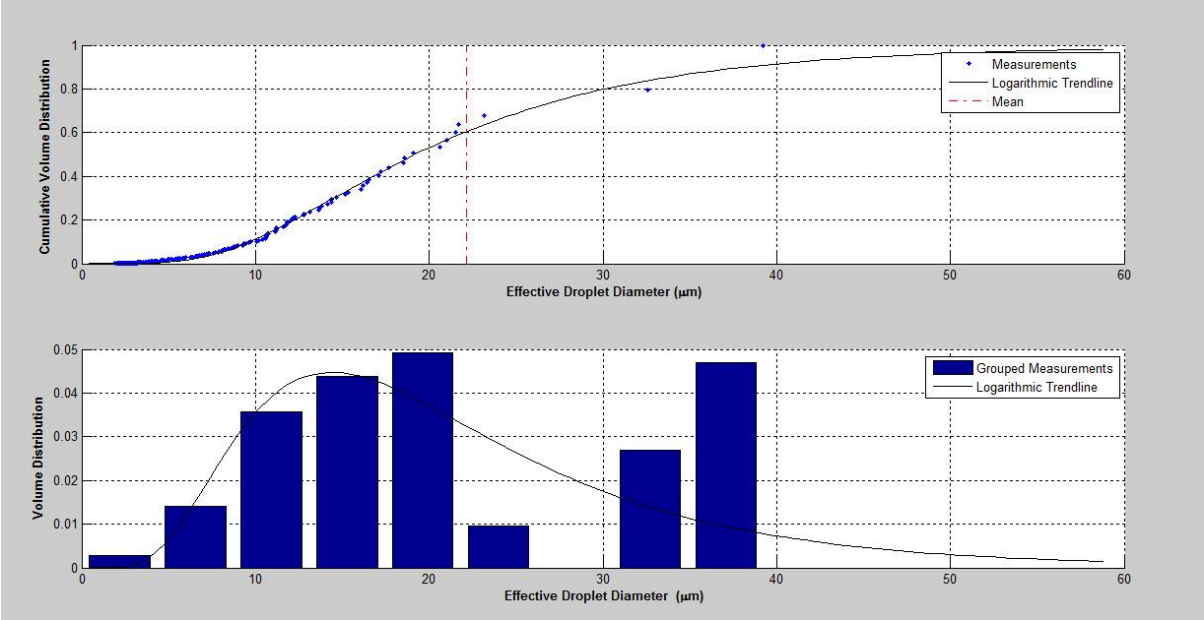

Figure 40: Average droplet size diameter for crude oil emulsion

As figures 39 and 40 demonstrate, the volume distribution of droplet in two emulsions has almost the same logarithmic trend confirming the similarity in the rheological behavior of these emulsions.

5. Conclusion

Potential benefits of using bio-oil emulsions for equipment development, testing and verification are high. It has also been substantiated that the environmental impact will be small. The proposed bio-emulsion showed promising rheological results with a large number of experimental stating its applicability for oil spill tests. Results also indicate the flexibility of bio-emulsion when it comes to adjusting viscosity values. Figure 39 shows the successful outcome of the studied test.

Figure 41: Oil spill test in Vesterålen islands, September 2014

6. References

AHMED, N. S., NASSAR, A. M., ZAKI, N. N. & GHARIEB, H. K. 1999. Formation of fluid heavy oil-in-water emulsions for pipeline transportation. *Fuel,* 78**,** 593-600.

ARAI, Y. 1996. Determination of powder characteristics. *Chemistry of Powder Production.* Springer Netherlands.

ASHRAFIZADEH, S. N. & KAMRAN, M. 2010. Emulsification of heavy crude oil in water for pipeline transportation. *Journal of Petroleum Science and Engineering,* 71**,** 205-211.

AZODI, M. & SOLAIMANY NAZAR, A. R. 2013. An experimental study on factors affecting the heavy crude oil in water emulsions viscosity. *Journal of Petroleum Science and Engineering,* 106**,** 1-8.

BARNES, H. A., HUTTON, J. F. & WALTERS, K. 1989. *An introduction to rheology,* Amsterdam, Elsevier.

CHENG, D. C. H. 1986. Yield stress: A time-dependent property and how to measure it. *Rheologica Acta,* 25**,** 542-554.

COULTATE, T. P. 2009. *Food: the chemistry of its components,* Cambridge, Royal Society of Chemistry.

FARAH, M. A., OLIVEIRA, R. C., CALDAS, J. N. & RAJAGOPAL, K. 2005. Viscosity of water-in-oil emulsions: Variation with temperature and water volume fraction. *Journal of Petroleum Science and Engineering,* 48**,** 169-184.

IGATHINATHANE, C., PORDESIMO, L. O., COLUMBUS, E. P., BATCHELOR, W. D. & SOKHANSANJ, S. 2009. Sieveless particle size distribution analysis of particulate materials through computer vision. *Computers and Electronics in Agriculture,* 66**,** 147-158.

IKOKU, C. U. & RAMEY, H. J., JR. Transient Flow of Non-Newtonian Power-Law Fluids in Porous Media.

JOSEFA, B.-R., XED, GUEZ, JOSEFA, B.-R., XED & GUEZ 2013. The Food Additive Polyglycerol Polyricinoleate (E-476): Structure, Applications, and Production Methods. *ISRN Chemical Engineering,* 2013.

LACROIX, C., ARESSY, M. & CARREAU, P. 1997. Linear viscoelastic behavior of molten polymer blends: A comparative study of the Palierne and Lee and Park models. *Rheologica Acta,* 36**,** 416-428.

MAIA FILHO, D. C., RAMALHO, J. B. V. S., LUCAS, G. M. S. & LUCAS, E. F. 2012. Aging of water-in-crude oil emulsions: Effect on rheological parameters. *Colloids and Surfaces A: Physicochemical and Engineering Aspects,* 405**,** 73-78.

MALASSAGNE-BULGARELLI, N. & MCGRATH, K. M. 2013. Emulsion ageing: effect on the dynamics of oil exchange in oil-in-water emulsions. *Soft Matter,* 9**,** 48-59.

MASALOVA, I., MALKIN, A. Y., SLATTER, P. & WILSON, K. 2003. The rheological characterization and pipeline flow of high concentration water-in-oil emulsions. *Journal of Non-Newtonian Fluid Mechanics,* 112**,** 101-114.

MERKUS, H. 2009. Particle Size, Size Distributions and Shape. *Particle Size Measurements.* Springer Netherlands.

MIRZADZHANZADE, A. K. 1990. Hydraulics for Petroleum Engineers.

NELSON, E. B. & GUILLOT, D. 2006. *Well cementing,* Sugar Land, Tex., Schlumberger.

OLAREWAJU, J. S. A Reservoir Model Of Non-Newtonian Fluid Flow. Society of Petroleum Engineers.

PAL, R. 1996. Effect of droplet size on the rheology of emulsions. *AIChE Journal,* 42**,** 3181-3190.

PAL, R. & RHODES, E. 1985. A novel viscosity correlation for non-newtonian concentrated emulsions. *Journal of Colloid and Interface Science,* 107**,** 301-307.

PAL, R. & RHODES, E. 1989. Viscosity/Concentration Relationships for Emulsions. *Journal of Rheology (1978-present),* 33**,** 1021-1045.

PETSEV, D. N. 2004. *Emulsons: structure, stability and interactions,* Amsterdam, Elsevier.

PRINCEN, H. M. 1983. Rheology of foams and highly concentrated emulsions: I. Elastic properties and yield stress of a cylindrical model system. *Journal of Colloid and Interface Science,* 91**,** 160-175.

RONNINGSEN, H. P. Correlations for predicting Viscosity of W/O-Emulsions based on North Sea Crude Oils. Society of Petroleum Engineers.

SHINODA, K. & FRIBERG, S. E. 1986. *Emulsions and solubilization,* New York, Wiley.

SKALLE, P. 2012. Drilling Fluid Engineering.

TADROS, T. F. 2005. *Applied surfactants: principles and applications,* Weinheim, Wiley-VCH.

TADROS, T. F. 2013. *Emulsion formation and stability,* Weinheim [Germany], Wiley-VCH.

WANG, W., WANG, P., LI, K., DUAN, J., WU, K. & GONG, J. 2013. Prediction of the apparent viscosity of non-Newtonian water-in-crude oil emulsions. *Petroleum Exploration and Development,* 40**,** 130-133.

7. Appendices

Appendix A

```
% LogNormal dråpefordeling
clear
clf
clc
load resultscrude4.xls
data=resultscrude4;
ant=size(data);
n=ant(1);      % antall målepunkter % Data points
disp([  '..............LogNormal  fordeling;  tilpVsning  til  målte
dråpedata.............'])
disp(['Antall målepunkter:     ',num2str(n)])
   A=data(1:n,2); % areal utreknet av ImageJ          %Second column in
the Excel file
   dfer=data(1:n,3); % Feret diameter                  %Third column in
the Excel file
    dfmin=data(1:n,4); %Minste Feret diameter         %Fourth column in
the Excel file
%
for i=1:n
V(i)=4/3*pi*(dfmin(i)/2)*(dfer(i)/2)^2;    % volum, rotasjonselipsoide
d(i)=(6*V(i)/pi)^(1/3);                              % gjennomsnittlig
dråpediameter     % Average Diameter
end
%  Empirisk fordeling
   Vs=sort(V);  % sorter dråpevolumer i stigende rekkefølge
   Vkum(1)=Vs(1);
   for i=2:n
   Vkum(i)=Vkum(i-1)+Vs(i);
   end
   Fe=Vkum/sum(Vs);  %  Fe(Vs)  =  empirisk  kumulativ  fordeling=empiric
cumulative distribution
   ds=sort(d);   % sorterer diametere i stigende rekkefølge=sort
%
%  Søylediagram  empirisk  sannsynlighetstetthet=Bar  Chart  empirical
probability density
nf=10;  % Antall søylet =  number of columns
dint=linspace(0,ds(n)*1.001,nf); % intervallinndeling=interval
for j=1:nf-1
   % grupper Volumlauke innen hvert diamerintervall=Volume Lauke groups
within each diamerintervall
   Vf(j)=0;
   for i=1:n
       if ds(i)>dint(j)& ds(i)<dint(j+1)
   Vf(j)=Vf(j)+Vs(i);
       end
   end
   dip(j)=(dint(j)+dint(j+1))/2;                % intervallmidtpunkt =
interval midpoint
   fe(j)=(Vf(j)/(dint(j+1)-dint(j)))/sum(Vs);         %         empirisk
sannsynlighetstetthet = empirical probability density
end

% ----------------LogN fordeling---------------------
```

```
    % Middelverdi og varians av målte data
   E=sum(Vs)/n;
   var=0;
   for i=1:n
        var=var+(Vs(i)-E)^2;
   end
   var=var/(n-1);
   Sd=var^0.5;
   disp(['Middelverdi av målte data  : ',num2str(E,'%5.3e\n')])
   disp(['Standardavvik av målte data: ',num2str(Sd,'%5.3e\n')])

   % Forventningsrette estimat av lokVsjons: mya, og skalaparameter: s2a
   my=log(E)-0.5*log(1+var/E^2);
   s2=log(1+var/E^2);
   disp(['Forventningsrett         estimat         av         my-parameter
',num2str(my,'%5.3e\n')])
   disp(['Forventningsrett         estimat         av         s2-parameter
',num2str(s2,'%5.3e\n')])
   %ML-estimat

   % utrekning av LogN-fordeling
   x=linspace(0.00,ds(n));

   for i=1:length(x)
   f(i)=(1/(2*s2*pi)^0.5)/x(i)*exp(-(log(x(i))-my)^2/(2*s2));
   F(i)=0.5*erfc(-(log(x(i))-my)/(2*s2)^0.5);
   end
    %
    %-----------------  optimer ---------------------------------
   global Feg xg

   Feg=Fe;           % empirisk kumulativ fordeling
   xg=ds;            % x-akse
   pa0= [my s2 ];   % initielt parameterestimat
   [pa,fval]=fminunc(@optfun,pa0);

      % Optimert estimat av lokasjons: mya, og skalaparameter: s2a
   myopt=pa(1);
   s2opt=pa(2);
   disp(['Lokasjonsparameter     optimert     fordeling                m=
',num2str(myopt,'%5.3e\n')])
   disp(['Skalaparameter    for    optimert    fordeling:         s    =
',num2str(s2opt^0.5,'%5.3e\n')])

   %  LogN-fordeling basert på optimerte parametre Distribition based on
   %  optimised parameters
   z=linspace(0.1,ds(n)*1.5);
   for i=1:length(z)
   fao(i)=(1/(2*s2opt*pi)^0.5)/z(i)*exp(-(log(z(i))-myopt)^2/(2*s2opt))
   Fao(i)=0.5*erfc(-(log(z(i))-myopt)/(2*s2opt)^0.5);
   end
    % ---------------------------
   % estimer middelverdi=estimated middle data
   x=linspace(0.01,10*ds(n),500);
   m=0;
   for i=2:length(x)
    m=m+x(i)*(1/(2*s2opt*pi)^0.5)/x(i)*exp(-(log(x(i))-
myopt)^2/(2*s2opt))*(x(i)-x(i-1));
   end
     %
```

```
subplot(2,1,1)
hold on
plot(ds,Fe,'.')
  plot(z,Fao,'k')
   plot([m m],[0 1],'r-.')
hold off
xlabel('\bf Effective Droplet Diameter (\mum)')
ylabel('\bf Cumulative Volume Distribution ')
grid
legend('Measurements','Logarithmic Trendline','Mean')
%axis([0 15 0 1 ])

 % tetthet
subplot(2,1,2)
hold on
bar(dip,fe)
%plot(dip,fe)
plot(z,fao,'k')
% plot([E E],[0, max(f)],'b-.')

hold off
xlabel('\bf Effective Droplet Diameter  (\mum)')
ylabel('\bf Volume Distribution')
grid
% axis([0 15 0 0.2 ])
legend('Grouped Measurements','Logarithmic Trendline')
```

Appendix B

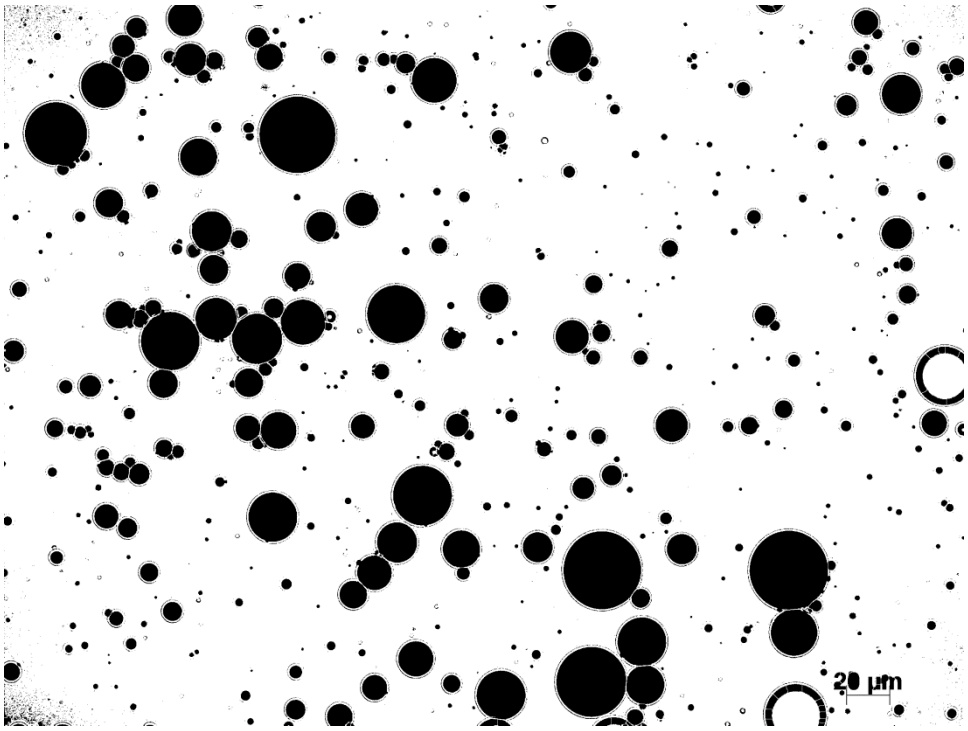

FigureA 1: Processed version of the figure37 where all holes are filled and split

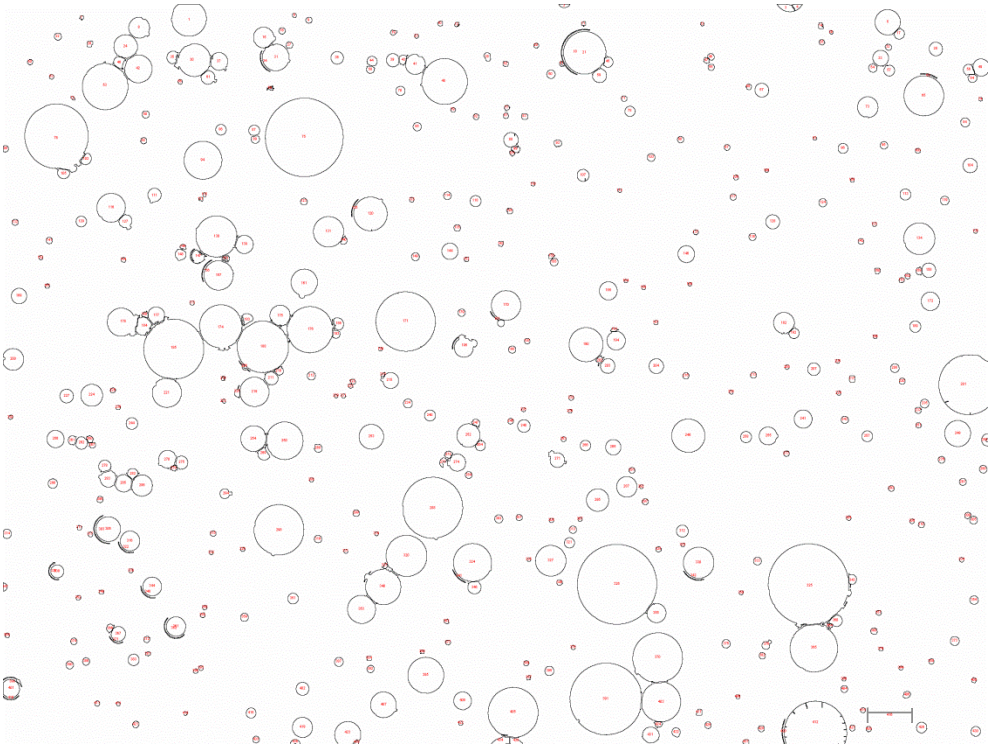

FigureA 2: Measured water droplets of figure 37and each particle is numbered

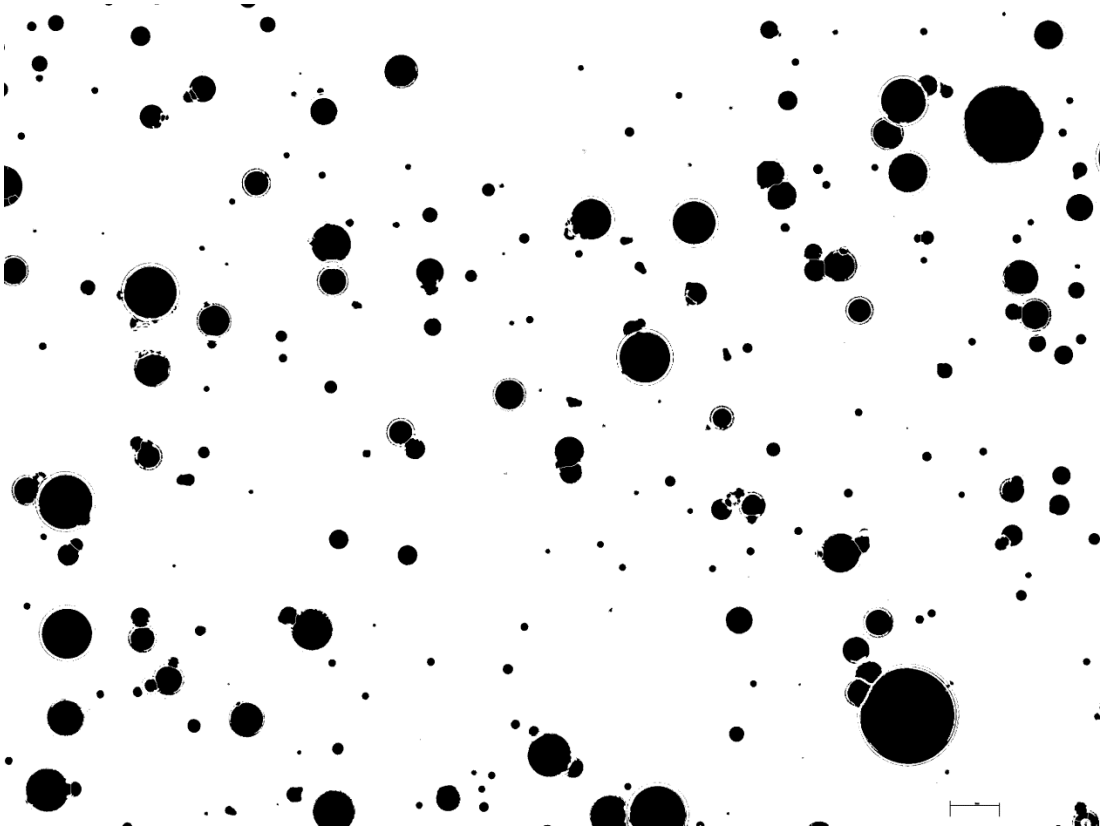

FigureA 3 Processed version of the figure38 where all holes are filled and split

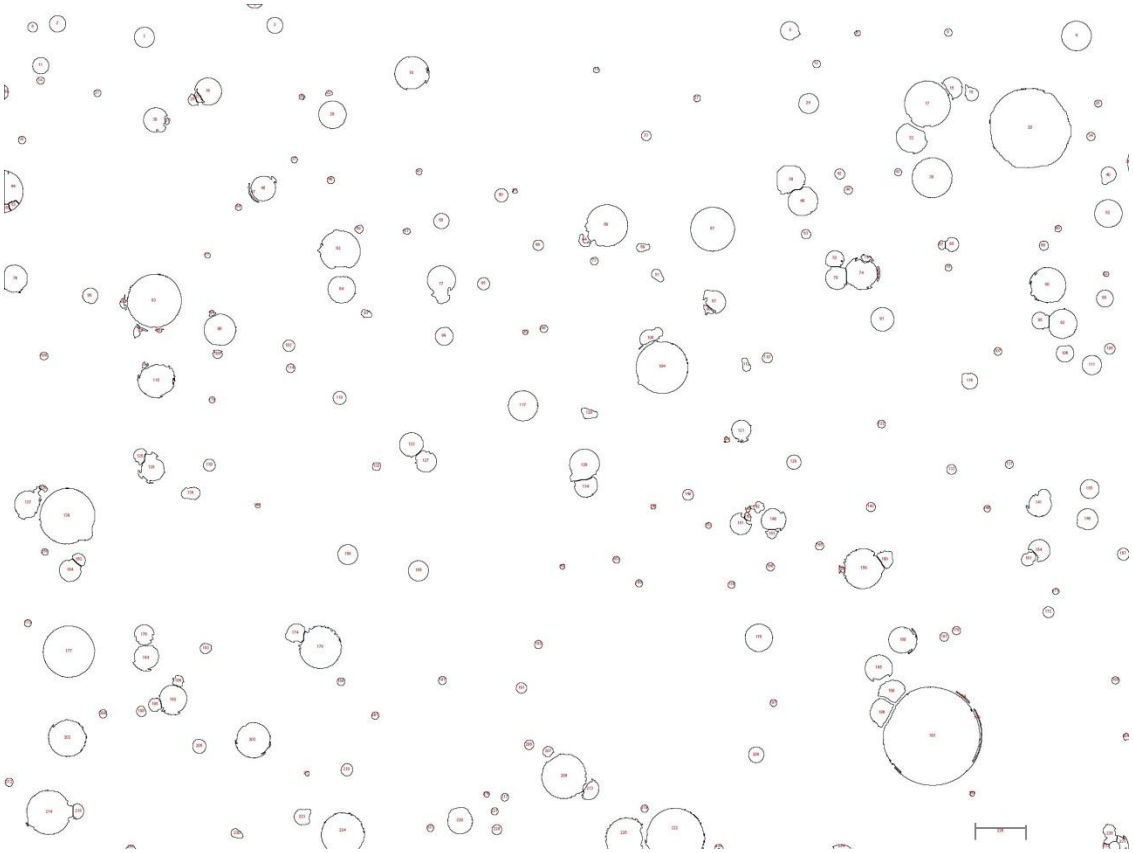

FigureA 4 Measured water droplets of figure 38 and each particle is numbered

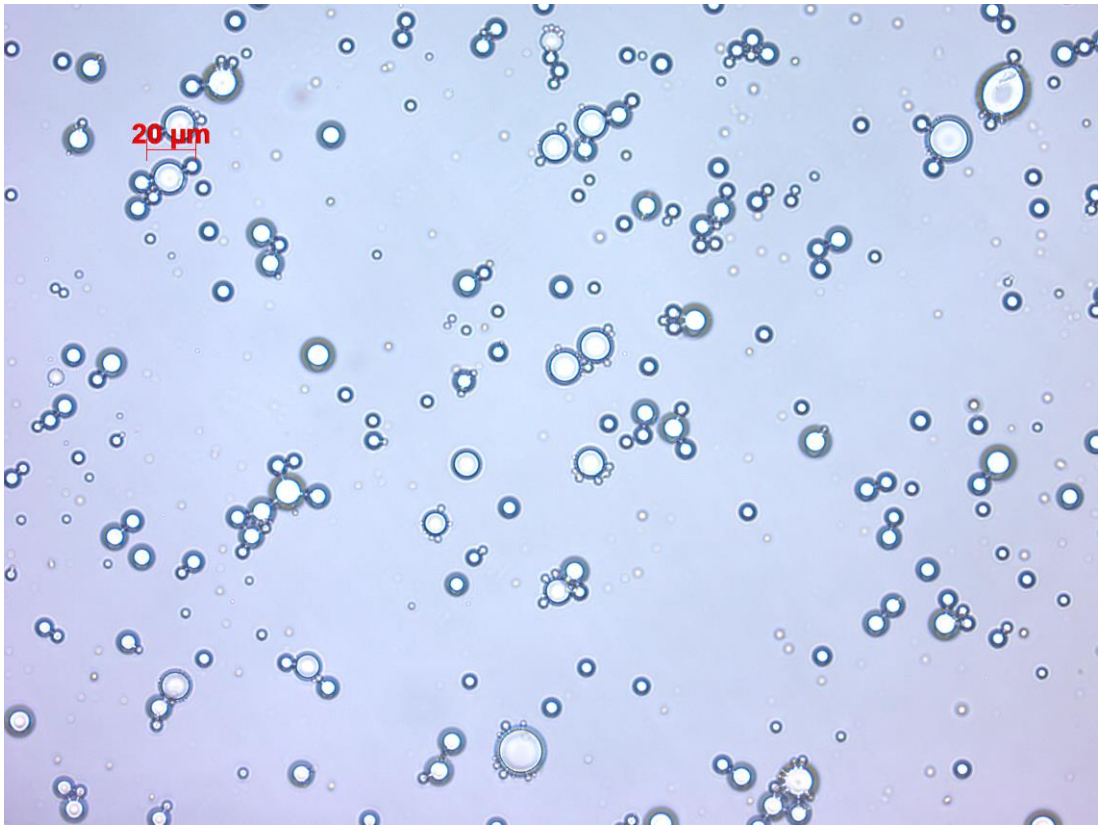

FigureA 5: Microscopic picture of bio-emulsion where blue colour added to the water phase

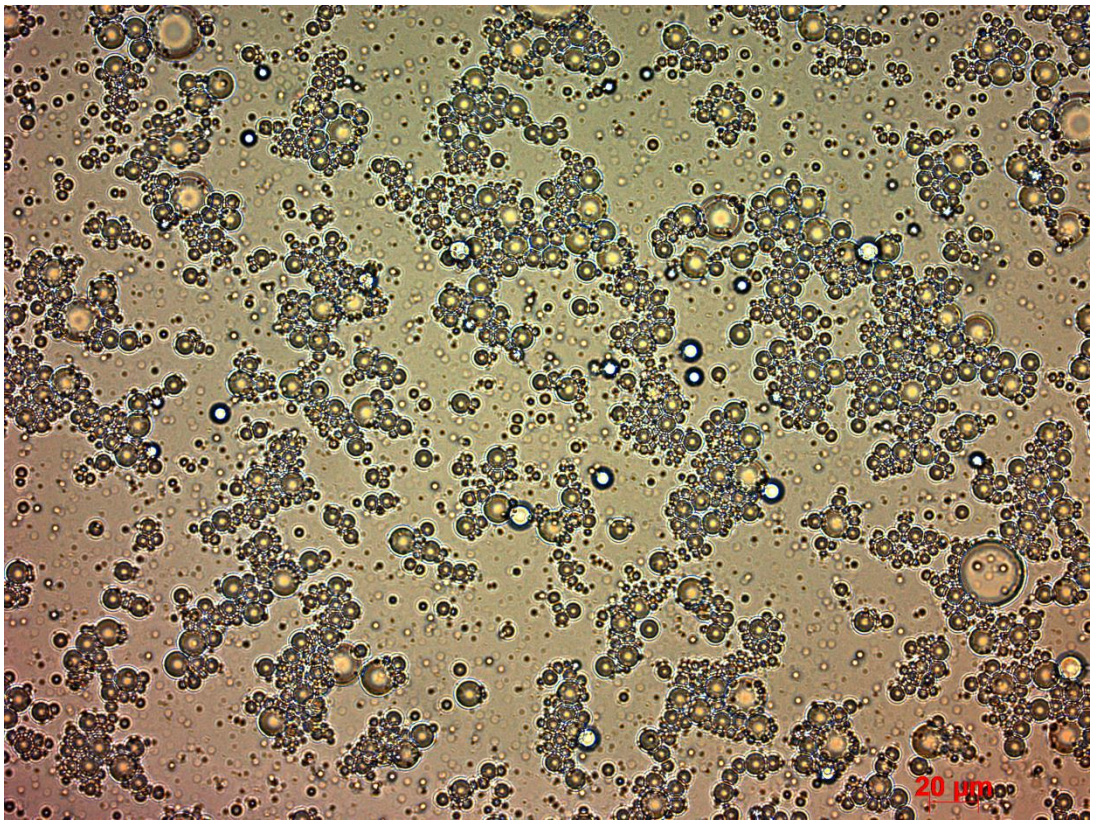

FigureA 6: Microscopic picture of bio-emulsion (90% water phase)n where no colour added to the water phase